An edited version of this paper was published by AGU
JOURNAL OF GEOPHYSICAL RESEARCH
DEC 2004; VOL 109; PART 12; SECT 3; pp. C12038; 2004
http://dx.doi.org/10.1029/2003JC002146

Hydrology and circulation in the Strait of Hormuz and the Gulf of Oman-Results from the GOGP99 Experiment: 2. Gulf of Oman

S. P. Pous[1,*], X. Carton[1], P. Lazure[2]

1 : Laboratoire de Physique des Océans, IFREMER/CNRS/UBO, Brest, France
2 : Direction de l'Environnement et de l'aménagement Littoral, Applications Opérationnelles, IFREMER, Plouzané, France

*: Corresponding author : Stephane.Pous@ifremer.fr

Abstract:

Hydrological, ADCP, and drifting buoy data obtained during the GOGP99 Experiment in October and early November 1999 are analyzed to describe the Persian Gulf Water (PGW) core and the regional circulation in the Gulf of Oman. The warm and salty PGW core flows out of the Strait of Hormuz heading southeastward unto (25°20′N, 57°E), approximately. From there, it cascades down the continental slope, veers southwestward, and joins the Omani coast near (24°50′N, 56°50′E) to form a slope current. This PGW current has then thermohaline maxima on isopycnal σ_0 = 26.5, near 220 m depth. Its thermohaline characteristics decrease along its progression to Ra's al Hadd (and then offshore into the Arabian Sea) but maintain a sharp contrast with surrounding waters. Outflow variability at the Strait of Hormuz can be related to downstream fluctuations of the thermohaline maxima in the PGW core at gulf scale and over a 2- to 3-week period. Moreover, several mechanisms (baroclinic instability, flow intermittency, cape effects) are examined to explain the widening of this PGW core upstream and downstream of Ra's al Hamra. In the eastern part of the Gulf of Oman, the regional circulation is a cyclonic gyre. The circulation in the western part of the Gulf is more complex, with the outflow of PGW and southeastward currents in the upper 250 m near the Omani coast, and a recirculation of upwelled waters near Ra's Jagin (on the Iranian coast). The large cyclonic gyre occupies at least the upper 300 m of the water column and undergoes little variation over a month. The PGW outflow in the northern Arabian Sea is southward and located 50–100 km from the coast. It borders a shallower northward current located offshore.

Hydrology and circulation in the Strait of Hormuz and the Gulf of Oman; results from the GOGP99 Experiment. Part II. Gulf of Oman

S. P. Pous, X. Carton, P. Lazure

abstract

Hydrological, ADCP and drifting buoy data obtained during the GOGP99 Experiment in October and early November 1999 are analyzed to describe the Persian Gulf Water (PGW) core and the regional circulation in the Gulf of Oman. The warm and salty PGW core flows out of the Strait of Hormuz heading southeastward unto $(25^o20'N, 57^oE)$ approximately. From there, it cascades down the continental slope, veers southwestward and joins the Omani coast near $(24^o50'N, 56^o50'E)$ to form a slope current. This PGW current has then thermohaline maxima on isopycnal $\sigma_0 = 26.5$, near 220m depth. Its thermohaline characteristics decrease along its progression to Ra's al Hadd (and then offshore into the Arabian Sea) but maintain a sharp contrast with surrounding waters. Outflow variability at the Strait can be related to downstream fluctuations of the thermohaline maxima in the PGW core at gulf scale and over two to three week period. Moreover, several mechanisms (baroclinic instability, flow intermittency, cape effects) are examined to explain the widening of this PGW core upstream and downstream of Ra's al Hamra.

In the eastern part of the Gulf of Oman, the regional circulation is a cyclonic gyre. The circulation in the western part of the Gulf is more complex, with the outflow of PGW and southeastward currents in the upper 250m near the Omani coast, and a recirculation of upwelled waters near Ra's Jagin (on the Iranian coast). The large cyclonic gyre occupies at least the upper 300 m of the water column and undergoes little variation over a month. The PGW outflow in the northern Arabian Sea is southward and located 50-100km from the coast. It borders a shallower northward current located offshore.

1 Introduction

The Gulf of Oman extends between 22 and 26^oN and 56 and 60^oE. In its northwestern part, it is connected to the Arabian/Persian Gulf (hereafter "the Gulf") by the Strait of Hormuz; in its southeastern part, it opens on the Indian Ocean and the Arabian Sea (see Figure 1). Shallow areas (bounded by the 200m isobath) are narrow along each coast (Omani and Iranian) and are wider in the vicinity of the Strait. Along the Omani coast, the continental slope is steep east of 58^oE; depths in excess of 3000m are found south of $24^o30'N$ and east of $58^o30'E$. Winds over the Gulf of Oman blow mostly along the northwest-southeast axis with seasonal variations (northwesterly winds are most common). Large evaporation rates over the Gulf lead to the formation of a warm and salty water mass (Persian Gulf Water, PGW) which flows into the Gulf of Oman through the Strait; the mass and salt budget in the Gulf are closed by an inflow of Indian Ocean Surface Water (IOSW) coming from the northern Gulf of Oman, and also by evaporation and by river discharge. Indirect estimates of this exchange flow through the strait (Sultan et al, 1993; Bower et al., 2000; Swift and Bower, 2003) suggested its high variability. More recently, data collected in the Strait of Hormuz show that, if the thermohaline properties of the water

masses undergo significant changes on the seasonal timescale, currents (at least of the outflowing PGW) have on the contrary remarkably low variability (Johns et al., 2003). At the head of the Gulf of Oman, the salinity of outflowing PGW is reduced by mixing with IOSW (Banse, 1997; Matsuyama et al., 1998; Swift and Bower, 2003). High rates of mixing are mainly attributed to topographic effects and to internal waves (with amplitudes reaching 20m).

Few in-situ experiments provide a synoptic view of the PGW core in the Gulf of Oman. Using CTD data from the Scheherazade experiment (RRS Charles Darwin, Feb-March 1997), Roe et al. (1997) have shown the rapid mixing of PGW exiting from the Strait, and the significant decrease in salinity maximum as this water core reaches its depth of neutral buoyancy. Downstream, they observed this PGW core with a 20 km width between 200 and 350m depths. Using the MOODS dataset, Bower et al. (2000) showed that downstream of the Strait, the PGW core flows southeastward along the Omani coast at 225m depth near $\sigma_0 = 26.5$ with temperature and salinity of about $20 - 22^oC$ and $37.5 - 38$ psu over the February-June period. In-situ measurements indicate that the PGW core can penetrate into the Arabian Sea (Rochford, 1964; Premchand et al., 1996; Prasad et al., 2001). The seasonal variability of the PGW core in the Gulf of Oman is still debated: using data from five surveys (R/V Dr Fridtjof Nansen, May 1975-Sept. 1976), Banse (1997) finds short-term variability but observes no obvious seasonality in the eastward advection of PGW. More recently, using data from 9 AXBT[1] surveys (Oct. 1992-March 1995), Bower et al. (2000) find seasonal variability of the PGW core (winter intensification of salinity, patchy structure of PGW in spring and fall, weaker temperatures in summer).

The regional circulation in the Gulf of Oman is not well known. The Admiralty Pilot (1982) notes that currents tend to flow cyclonically in the Gulf of Oman. From surface drifting buoys (February 1992), Reynolds et al. (1993) observe a double gyre circulation pattern, with an anticyclonic loop near the Strait, and cyclonic rotation between $58^o30'E$ and 60^oE; in between, a cold patch extends southward from the Iranian coast. But this regional circulation is subject to notable variability including eddies (Quraishee, 1984; Reynolds, 1993; Bower et al., 2000). High-resolution infrared images of NOAA-6 show mesoscale structures near the surface during the SW monsoon (Cagle et al., 1981). Seasonal variability of currents near Ra's al Hadd was identified by Flagg et al. (1998), using 18 months of SADCP[2] data (between 1994 and 1995). From January to July, currents along the northeastern Omani coast were rather slow ($O(0.1 - 0.3m/s)$) with a trend for northerly flow. In August 1995, a flow reversal appeared with stronger southeasterly currents ($O(0.8m/s)$). Flagg et al. surmise that this flow reversal is related to the intensification and/or the propagation of a cyclonic eddy in the Gulf of Oman in response to the monsoon. They also suggest that currents near Ra's al Hadd may be a conduit for the PGW core during the period of strong southerly flow. A seasonal influence of monsoon regimes on currents in the Arabian Sea is described by Prasad et al. (2001).

To characterize the PGW outflow and the regional circulation, the French Navy Hydrographic and Oceanographic Service (SHOM) conducted an experiment in October 1999 (GOGP99) in the Strait of Hormuz and in the Gulf of Oman. CTD[3] sections with LADCP[4] or SADCP measurements, Seasoar[5] transects and AXBT/AXCTD[6] casts provided repeated information on the hydrological and dynamical structure of the PGW core and on the regional circulation. Surface drifting buoys drogued at 15, 50, 85 or 230m followed these currents. All these data also provide information on the short-term variations

[1] Air-dropped expendable bathythermographs

[2] Shipborne Acoustic Doppler Current Profiler

[3] see definition of CTD, XBT, XCTD in part 1 of the paper

[4] ADCP used in Lowered mode

[5] Underwater vehicle towed behind the ship at approx. 7-8 knots, equipped with SBE911+ CTD probe and Wetstar fluorimeter, and following an undulating trajectory in the vertical plane, between 10 and 300m depths

[6] XBT or XCTD probes dropped by airplane

of these currents.
After recalling the data collection and processing (section 2), the hydrological structure, the pathways and dynamical structure of the PGW core are analysed (section 3). The short-term variability revealed by Surdrift buoys, by hydrological and ADCP data is described. The following section presents the regional circulation in the Gulf of Oman at various depths. Finally, the main results are summarized and conclusions are presented.

2 Data collection and processing

The GOGP99 experiment was conducted by SHOM in the Strait of Hormuz and in the Gulf of Oman from October 8 till November 10, 1999. During GOGP99, 243 CTD stations, XBT or XCTD casts, forming 16 sections, twelve Seasoar transects in the upper 300m of the water column and 25 AXBT and AXCTD soundings using an "Atlantic2" patrol plane of the French Navy, constituted 3 hydrological networks in the Gulf of Oman (see Figure 2 and Table 1 for the location and dates of sections). SADCP measurements accompanied all hydrological transects.
The first hydrological network included 131 CTD, XBT, XCTD and LADCP stations (Oct. 8-16). The second hydrological network comprised 35 CTD, XBT and XCTD stations, 4 Seasoar transects and 25 AXBT, AXCTD casts (Oct.21-26). The third hydrological network had 8 Seasoar transects, and 43 CTD and XBT stations (Oct. 29-Nov. 02). Finally, a single CTD/LADCP, XBT, XCTD section (32 stations) was performed in the Arabian Sea at the end of the experiment (Nov.10).
Among these stations, 33 constituting 3 sections (R18a,b,c) were already described in Part 1 of the paper, but are recalled here to illustrate the initial outflow of PGW from the Strait of Hormuz.
Finally, four surface drifting buoys (Surdrifts) drogued at 15, 50 or 230m were launched at the head of the Gulf to follow the IOSW or PGW currents and eddies (see Table 4 for their deployment positions and for their characteristics); two other Surdrift trajectories, drogued at 15 and 85m, already described in Part 1 of the paper, are recalled here for completeness.

Quality checks, calibration and filtering were applied to the data[7].
Hydrological profiles were first calibrated on in-situ measurements (surface temperature and chemical analysis of salinity from water samples). Then, a median filter was applied and spurious points were eliminated by visual inspection of each profile. A Newtonian binomial smoothing was then applied to reduce the number of points to 10 to 20% of initial number, under the condition that the initial (filtered) profile could be reconstructed via linear interpolation with a minimal error. CTD accuracy is $\pm 0.003^oC$ on temperature, ± 0.005 psu on salinity, ± 1 dbar on pressure; XBT/XCTD accuracy is $\pm 0.05^oC$ on temperature, ± 0.03 psu on salinity, $\pm 5m$ on vertical position of the probe. Hydrological sections were visualized within Ocean Data View software (Schlitzer, 2003).

Seasoar data used here are only CTD measurements which have been processed as described above. Vertical precision is $\pm 1m$. LADCP was a 150 kHz RDI instrument and SADCP a 76 kHz instrument. SADCP data cover the 0-300m depth range, and LADCP data the 0-1000m one. LADCP data was integrated over 8m vertical bins. Precision over LADCP and SADCP measurements is respectively $\pm 0.04m/s$ and $\pm 0.05m/s$.

Finally, Surdrift buoys were positioned by GPS with a 100m horizontal accuracy. Trajectories were re-sampled every hour with a three-day window filtering. Tests were performed on acceleration to detect possible loss of drogues or trawling. In such cases, trajectories were ended. The Surdrift buoys are not exactly Lagrangian floats since the drag exerted by the upper water masses on the cable linking the surface float to the deep drogue contributes to the mo-

[7] details are given in Vrignaud, Du Reau et al. and Michaux technical reports (2000) which can be obtained from EPSHOM/CMO, 13 rue du chatellier, 29200 Brest, France

tion. For drogues lying at depth ranging between 15 and 230m, simple calculations can show that this drag is less than one tenth of the drag exerted on the drogue. Moreover, the large dimensions of this drogue sometimes cause the stranding of the buoy.

3 Structure and variability of the PGW outflow in the Gulf of Oman

The hydrological sections performed during the GOGP experiment sampled the whole Gulf of Oman between October 8 and November 10 1999; their positions are shown on Figure 2. Information concerning the 31 sections is given in Table 1. Sections were achieved from the Omani coast towards the limit of Iranian waters. Since our study focuses on the hydrological of PGW in the Gulf of Oman, only the upper 300m of all sections are described.

3.1 Hydrological characteristics of PGW core and mixing with neighboring water masses

In the whole Gulf of Oman, our observations confirm that the PGW outflow is characterized by salinities larger than 37 psu and by temperatures higher that 20^oC in sharp contrast with the surrounding waters. In particular the salinity difference with surrounding waters is always larger than 1 psu. This enables the identification of a PGW core from the Gulf to the Arabian Sea (see also vertical sections on figures 6-9 and isopycnic maps on figures 14 and seq.):
from source waters with temperature 27^oC and salinity 39.75 psu in the Gulf, a noticeable decrease of both temperature and salinity maxima occurs over 150 km in the Strait of Hormuz (see figure 3, and table 2 to relate distances from R13 to section names): the PGW core in the northern Gulf of Oman has $T = 26^oC$ and $S = 38.5$ psu on section R18c on the shelf (close to shelfbreak). Then, a sharp decrease in temperature is observed just downstream of this location, as the PGW outflow starts falling down the continental slope; indeed, section R17 exhibits thermohaline maxima with $T = 23^oC$ and $S = 38$ psu, 35 km downstream of R18. These values remain nearly constant from there to section R14/S06 (located near $24^oN, 57^o30'E$, upstream of Ra's al Hamra). From R14/S06 to R04/S01, i.e. over 125 km, the PGW outflow experiences again a sharp decrease in temperature, down to 21^oC. A temperature minimum of 20^oC and salinity minimum of 37 psu are observed on R02. Finally PGW temperature and salinity in the Arabian Sea (section R01) are close to 21^oC and 37.1 psu.

The various hydrological sections have just shown that substantial decrease of thermohaline characteristics occur (a) in the Strait of Hormuz, (b) at shelfbreak in the northern part of the Gulf of Oman, (c) shortly upstream and downstream of Ra's al Hamra. The third event will be interpreted later in terms of mesoscale dynamics. The first two events are now interpreted as the turbulent mixing of PGW with surrounding waters. This turbulent mixing can be due either to wind variability and to bottom friction (especially in the shallow strait), or to intense internal waves (in particular at shelfbreak, see part 1 of this paper), or else to the cascade of the PGW outflow from the continental shelf (80m depth) to its depth of neutral buoyancy (roughly 220m).
To quantify this mixing, we have to define the water masses near PGW in the Strait and near shelfbreak. In the Strait, the surrounding water is IOSW with characteristics $T = 22^oC$, $S = 36.5$ psu. When PGW cascades down the continental slope, it mixes with surrounding waters between 100 and 250m. Average temperature of 19^oC and salinity of 36.75 psu are found on the various sections as representative of the water masses there, and also slightly downstream near 200m depth.
Therefore, a first mixing line is plotted to connect the source PGW water (on section R13), the PGW at the exit of the Strait (on section R11) with the surrounding IOSW (figure 4). This line is nearly straight; thus PGW at the exit of the Strait can be considered as source PGW mixed with IOSW in the strait. The second mixing line connects this PGW at the exit with the deeper surrounding water near the shelfbreak (as defined hereabove). Thermohaline characteristics of

PGW observed on sections R17, 16 and 15 fall on this line. This shows that PGW mixes with the deeper water (near 200m depth) of the Gulf of Oman as it falls down the continental slope.
Concerning PGW mixing with surrounding water masses, an interesting comparison can be drawn with previous work based on a streamtube model (Bower et al., 2000). Their figure 7a shows the positions of the T and S maxima of PGW near shelfbreak. Our section R19 is 5km upstream of the source point of this trajectory, our section R18 intersects it at kilometer 40 and our section R17 is located 15km downstream of the final point of this line. Our data indicate that the T and S peaks on R18 fall on this line; they also show a southeastward progression of T and S maxima from R19 to R17.
Comparing now our figure 3 and their figures 7c,d shows that the amplitude and location of thermal decrease closely correspond: a 3^oC decrease in both cases, between kilometers 50 and 60 for Bower et al., and between kilometers 40 and 75 in our data. On the contrary, our data show a less marked salinity decrease near shelfbreak than in Bower et al. (0.5 psu instead of 2 psu) because salinity has already strongly diminished in the Strait.

It must be noted finally, that once the PGW core has left the continental shelf, it is separated vertically from the warm and salty thermocline waters (which lie in the upper 30 meters) by a layer of cold and fresh IOSW, with thickness ranging between 100 and 120m. The ADCP velocity data shows that the currents near the northeastern Omani coast[8] bear southeastward with a slight decrease from the surface: currents larger than $0.3m/s$ are found near the thermocline (locally reaching $0.5m/s$ near the mouth of the Gulf of Oman) while the PGW core flows at $0.2m/s$ (with local maxima at $0.4m/s$).

[8]more precisely, near the 200m isobath since data very close to the coast were not available

3.2 Pathways, geometrical characteristics and spatial variability of PGW

To determine the position and geometrical characteristics of the PGW outflow in the western and eastern parts of the Gulf of Oman, its thermohaline characteristics and those of surrounding waters were examined. First, we analyze the depth of maximum salinity. This salinity maximum decreases downstream, but always maintains a 1 psu difference with surrounding waters (which lie either above in the Strait, or at 200m depth along the Omani coast). Therefore we define the half sum of these two values of salinity (PGW maximum and neighboring waters) as the isohaline bounding the PGW core. Thus we determine its width and thickness. The evolution of PGW depth, width and thickness from source to the Arabian Sea are presented on figure 5.

The depth of the PGW outflow evolves as follows[9]. The PGW core flows over the seabed in the Strait of Hormuz and over the shelf in the northwestern part of the Gulf of Oman (at depths increasing from 70 to 120m). Between sections R18 and R17, the PGW outflow leaves the seafloor and sinks to 200m depth, where it reaches neutral buoyancy (see also figures 6a-b). This variation in depth is naturally related to those in temperature and salinity shown on figure 4. The maximum decrease in temperature occurs when the PGW outflow sinks and the effect of turbulent mixing seems very localized. After section R17, the PGW core remains near 200m depth over nearly 200km (but at R15 where it is slightly shallower). This can also be correlated with the nearly constant temperature and salinity over this part of its path, indicating that the PGW core has reached equilibrium. Over the 300km from R14 to R02, the PGW core depth and salinity vary little (the depth rises by less than 30m), while its temperature still decreases by 3^oC. This temperature decrease renders the outflow denser; this is compatible with a rising of its level if it encounters denser water near the mouth of

[9]for all plots of figure 5, values on section R12 were discarded to avoid spurious variations due to the presence of the bottom trench and to the narrowness of the section

the Gulf of Oman.

Using the isohaline $(S_{max} + S_{env})/2$ as the PGW core boundary, its width and thickness are determined and exhibit the following variations:

The PGW core remains narrow and thin down to section R18, inshore of shelfbreak; the PGW width is then on order of 30-35km, its thickness on order of 30-40m. Assuming a PGW outflow transport of $0.15Sv$ in this area (Johns et al., 2003) leads to average velocities of $0.15m/s$. And indeed section R13 showed geostrophic velocities close to $0.1m/s$ over 30km width, with a narrow peak at $0.4m/s$, 5km wide (see part 1 of the paper); the geostrophic and estimated currents have thus similar magnitudes. After section R18, the PGW core undergoes considerable vertical stretching and noticeable lateral spreading as it falls down the continental slope: its width doubles (to 60km) and its thickness triples (to 100m) from section R18 to section R17. Further downstream, the PGW core thickness does not vary much, but for a slightly thicker core at sections R14/R07/S06 (these sections lies nearly at the same location upstream of Ra's al Hamra), and a slightly thinner core at R02 (at the mouth of the Gulf of Oman).

The variations in width of the PGW core are more instructive. After its spreading at R17, the PGW core regains a narrow shape along the Omani coast at R16 and R15 (roughly 30km wide). Upstream of Ra's al Hamra, at section R07/R14/S06, the PGW core widens to 60km offshore; this widening is again observed on section S05 (figures 6c-d) before the PGW flow narrows at Ra's al Hamra. This widening of the PGW core has already been observed in historical data at nearly the same location by Bower et al. (2000). They describe a large meander of PGW, upstream of Ra's al Hamra, in June 1993, May 1994, and a weaker one in November 1993, and in December 1994. On Plate 10 of their paper, these meanders have a wavelength close to 100km. Here, the spacing of our sections can only give a larger upper bound (180km) for this wavelength.
In the appendix, several mechanisms (baroclinic instability, influence of time-varying outflow, influence of bottom slope) are examined for the existence of this meander. Within its limits of applicability (neglecting too steep topographic slopes), the linear quasi-geostrophic model yields most unstable wavelengths close to those observed in-situ. A time-varying transport of the outflow could also account for the accumulation of water in a meander. On the contrary, the effect of a bottom slope is rather stabilizing. All these mechanisms should nonetheless be examined with finer-scale data and information on PGW transport or potential vorticity near the coast.

At Ra's al Hamra (section R05), the PGW core is very narrow (20km wide). This can be due to the local convergence of currents (regionally) or to a cape effect (see hereafter). Downstream of Ra's al Hamra, we observe again a widening of the PGW core (see section R04 on figure 7a and section S01 on figure 8a) that we attribute to the effect of the cape. Following Boyer and Tao (1987) and Davies et al. (1990), we idealize this cape and the neighboring isobaths as a triangular spur of offshore extent $D = 35km$ (estimated from the 200m isobath 100km upstream and downstream of the cape), with depth $H = 300m$. Following these authors, and using a density difference of $1kg/m^3$ between 100 and 300m depth, the stratification parameter is $S = NH/f_0D$ close to unity (or slightly less) and the Rossby number is $Ro = U/f_0D$ close to 0.1 (or slightly more). With such dimensionless numbers, Boyer and Tao (1987) showed experimentally that a uniform flow encoutering a cape produces anticyclones in its lee. These anticyclones remain attached to the cape (and produce a widening of the flow) for S smaller than or close to unity and large Reynolds number, whereas they detach and migrate downstream for larger S and for small Reynolds number.
On section R04, at the level of the PGW core, SADCP data show that velocity increases from the coast offshore, indicating anticyclonic vorticity (see figures 7a-b) as predicted by theory.

At the mouth of the Gulf of Oman, on section R02, the PGW core is narrower (35km wide) and maximal

velocities (close to 0.4 m/s) are found near the coast (see figure 9b). But this coastal core is attached to a wider, more diffuse and shallower filament of salty water extending from 23^oN to $23^o45'N$ (figure 9a). The SADCP section evidences intense horizontal velocity shear near $23^o15'N$, with outflow south and inflow north. This shear may be responsible for the tearing of the filament from the coastal PGW core. Finally the widening of the PGW core in the Arabian Sea (section R01) is due to the presence of two thermohaline maxima, the more intense one being at 100km offshore and the weaker one 40km away from the coast. The large distance of the intense PGW core from the coast can be attributed to the centrifugal acceleration around Ra's al Hadd. The splitting of the PGW core into two branches can be due to the presence of a northward current offshore (near 61^oE) and of one close to the coast and intensified below 200m depth.

3.3 Short term variability of the PGW core

A few hydrological sections were repeated several times to evaluate PGW outflow variability at periods close to two weeks. Section R18, in the northwestern Gulf of Oman, shows a temperature and salinity decrease of the PGW core on a ten day period. This decrease is also present downstream, near $57^o30'E$, between October 9 and 26 (sections R07, S06, R14). Further south, near $58^o30'E$, thermohaline maxima of PGW increase from October 11 to October 25 and decrease thereafter to October 29 (sections R05, A05, S02). Finally, increase of T and S maxima from mid to end October are seen both at 59^oE (sections R04, S01, figures 7a and 8a), and at 60^oE (sections R02, A02). In summary, the trend is a decrease of thermohaline maxima near the Strait, an increase near the mouth of the Gulf of Oman, and a mixed variation in between.

A first explanation for this evolution could be variations of the outflow of PGW at the Strait associated with advection. With a $0.2m/s$ velocity for the PGW core, the travel time would roughly be 9 days between sections R18 and R07, 6 days from R07 to R05 and 9 days between sections R05 and R02. These advective timescales are compatible with the time intervals between the observed variations.

Another explanation for these variations could be meander growth and/or eddy detachment from the PGW current, which can locally induce a noticeable decrease of the flux. This explanation is supported by the observation of meanders on the PGW core (see above) and by looping trajectories of floats near the PGW core (see below).

A third mechanism responsible for spatial variability of thermohaline properties of the PGW core could be the diffusion of heat and salt into the adjacent water masses. In particular, since PGW was warmer in the Gulf and upper water masses were colder in the Gulf of Oman in mid-September (see K10 SST maps in Part 1 of the paper), increased temperature gradients between the PGW and the adjacent water masses could have lead to more efficient diffusion, south of the Strait of Hormuz.

3.4 Drogued buoy trajectories in and near the PGW core

Surdrift trajectories provide information on the currents at depths ranging from 15 to 230m depths in the northern Gulf of Oman, and on the PGW core path and instabilities (see Figure 12). Firstly we recall that buoys 14979 (drogued at 85m) and 14677 (drogued at 15m) achieved an anticyclonic loop of 25-30 km diameter near $25^o30'N - 57^oE$. At 85m depth, this loop can be interpreted as an eddy of the PGW current which could be generated by an upslope displacement of this core (the squeezing of water column generating negative relative vorticity). At 15m depth, no direct current measurement is available. The closest recordings come from mooring D1, the shallowest measurement level of which is 27m (see part 1 of the paper). Currents at 27m depth fluctuate with periods varying between 3 and 8 days (on the order of wind fluctuation periods), and are fairly weak (slower than 0.1 m/s), except during the episode of strong southward flow from October 22 to 29. Therefore it is difficult to determine exactly the dynamical origin of the buoy loop at 15m.

Buoy 14932 (drogued at 230m) launched nearby, headed towards the PGW outflow but got stranded

after crossing the 200m isobath, and thus did not provide much information. Buoy 14697 (drogued at 15m), launched near the Iranian waters, roughly followed a southward route, with an average velocity between 0.15 and $0.2m/s$.
Buoy 14800 (drogued at 50m) launched at the head of the Gulf, first underwent one and a half counterclockwise loops with roughly 40 km diameter, indicating a cyclonic meander of the flow above the PGW core (see also 3.2). Downstream, buoy 14800 drifted above the PGW path at speeds varying between 0.15 and $0.45m/s$ covering 950 km in 35 days. After veering south at Ra's al Hadd, it escaped 70 km offshore in the Arabian Sea, flowing above the PGW core measured on section R01.
Buoy 14824 (drogued at 230m) was launched in a patch of PGW located near the Iranian waters $(25^o10'N, 58^oE)$. Two perpendicular hydrological sections indicate that this patch has $T = 21^oC, S =$ 37.75 psu, a meridional extent of at least 10 km but a longer zonal extent (at least 15 km with two cores). Thus, this patch resembles a filament. Buoy 14824 trajectory was not trapped in this filament and performed a large cyclonic loop at about $0.15m/s$ to enter the PGW core near the Omani coast, following then closely the 200m isobath.

4 General circulation and regional features in the Gulf of Oman

Figure 13 presents the T-S diagram in the Strait of Hormuz and in the Gulf of Oman, obtained with the GOGP99 data. These data have been gathered in three regions, (I) north of $25^o40'N$ and between 55^oE and $57^o50'E$, (II) south of (I), north of $23^o30'N$ and between the same longitudes, (III) north of 22^oN and between $57^o50'E$ and 62^oE (see also figure 1). Five main water masses can be observed on this diagram:
- the seasonal thermocline waters, TW, lying in the upper 25 m and formed during summer, with $T \sim 30^oC, S \sim 37$ psu,
- the Indian Ocean Surface Water, IOSW, lying between 50 and 100m depths, with $T \sim 20 - 22^oC, S \sim 36 - 36.5$ psu,
- the Persian Gulf Water in the Gulf of Oman, PGW, between 150 and 300m, with $T \sim 20 - 22^oC, S \sim 37.25 - 37.5$ psu (note that the PGW water in the Strait has $T = 27^oC, S - 39.5$ psu),
- the Red Sea Water, RSW, near 800m depth, with $T \sim 10 - 12^oC, S \sim 35.5$ psu, which can be seen only in regions (II) and (III) as expected,
- the North Indian Deep Water, NIDW, between 2000 and 4000m depths, with characteristics $T \sim 2^oC, S \sim$ 34.8 psu (see Tchernia, 1978). It is found only in region (III).
Considerable mixing occurs in the upper 300m, either due to the wind and tidal processes in the Strait or to turbulent diffusion along the PGW core. The T-S diagram is quasi-linear for temperatures lower than $15 - 16^oC$, i.e. below 400m depth.

4.1 Thermohaline characteristics and currents near the thermocline

Figure 14a shows the distribution of salinity on the isopycnic surface $\sigma_0 = 23.75$ at the base of the seasonal thermocline. The depth of this surface is also shown (figure 14b) as well as the horizontal currents at the average depth of this surface (20m; figures 14c and d). Firstly, it must be noted that all data (whatever the date of their collection) were used to produce the isopycnic maps of salinity (to obtain sufficient spatial resolution). Considering that some hydrological properties (e.g. those of the PGW core) varied between the beginning and the end of the GOGP99 experiment, the present maps provide only an average structure of the water masses, and their quasi-stationary features.

Clearly, warm and salty water flows out of the Strait of Hormuz over the continental shelf (and offshore to isobath 500m), north of 25^oN and west of $57^o40'E$. This water mass has temperature close to $28.5 - 29^oC$ and salinity above 37 psu (Figure 14a). Several warm and salty water patches (with temperature 28^oC and salinity 36.8 psu) are found along the Omani coast; in particular, one is found upstream and one downstream of Ra's al Hamra. These patches are separated by colder and fresher

ponds (for instance near $24^o15'N, 57^oE$, or near $23^o45'N, 58^o20'E$). The depth of the isopycnal $\sigma_0 = 23.75$ in the southern Gulf of Oman is 20-25m (figure 14b). The currents at 20m depth in the southwestern Gulf of Oman roughly follow the 200m isobath (and are thus directed southeastward) (figures 14c and d).

The position of velocity maximum exhibits variations between $57^o30'$ and 58^oE; this maximum can be either along the 200m isobath or 50 km offshore (figures 14c and d). On the westernmost section of both SADCP and LADCP networks[10], the surface currents near the shelf (and the strait) are maximum along the 200m isobath. Their intensity fluctuates geographically, with values larger than $0.3m/s$ near the shelfbreak; these currents can reach $0.5m/s$ between Ra's al Hamra and Ra's al Hadd. The southward currents at thermocline level near the shelfbreak suggests the presence of an outflow of surface water from the Strait. Farther downstream, at $24^oN, 57^o30'E$, an anticyclonic motion is clearly seen near the 200m isobath (in both ADCP networks), in close correlation with the anticyclonic meander on the PGW core 200m below. At that location, the southeastward flow has its maximum 50km away from the shelf (above the rim of the PGW core meander).

Downstream of Ra's al Hamra, a pool of warm and salty water corresponds to southeastward currents spreading at least 50 km offshore in both ADCP networks (figures 14c and d). In the LADCP network, the maximum velocity comes back closer to the coast at Ra's al Hadd, suggesting an anticyclonic region in the lee of Ra's al Hamra (figure 14d).

In the Arabian Sea, the current is southward at the location of the PGW core (near 60^oE) and northward offshore (near 61^oE).

Near the Iranian coast, a colder and fresher water patch (27.5^oC, 36.4 psu) lies between $58^o45'E$ and $59^o15'E$ north of 25^oN (near Ra's Jagin); currents circle it anticyclonically. Though cold and fresh water is advected westward along the Iranian coast, the $\sigma_0 = 23.75$ surface rises by nearly 10m at this cold patch, suggesting that it may be an upwelling. To support this hypothesis, we have analyzed the 0.5^o-resolution Quikscat winds (from CERSAT, provided by Dr Bentamy); they reveal a long episode of eastward/southeastward winds in the northwestern Gulf of Oman from October 16 till 20. We also analyze the currents near $25^oN, 59^o15'E$: they are westward/northwestward between October 8-13, but southwestward between October 21 and November 1. Therefore, an upwelling must have apeared or amplified between October 13 and October 21, in agreement with the episode of eastward/southeastward winds. Offshore of this coastal patch, a small fragment of cold water has detached and lies near $24^o45'N, 58^o15'E$. Unfortunately, no velocity data across this fragment are available to determine its dynamics.

The general circulation in the Gulf is cyclonic, at least very clearly so between 24^oN and 25^oN and between $58^o30'E$ and 60^oE. In the SADCP network (figure 14d), the circulation between 24^oN and 25^oN and $56^o30'E$ and 58^oE is also cyclonic but with weaker currents and not as a closed gyre. The LADCP network also shows the cyclonic circulation in the eastern part of the Gulf of Oman (figure 14c).

4.2 Characteristics and dynamics of water masses at 100 m depth

Figure 15a shows salinity on isopycnal $\sigma_0 = 25.75$ located near 100m depth (see figure 15b). Figure 15a clearly shows the thermohaline front south of the Strait of Hormuz (already described in Part 1). The horizontal gradients reach 0.06^oC/km and 0.03 psu/km. Downstream, warm and salty water extends along the Omani coast and into the Arabian Sea. A cold and fresh meander is observed near $24^o30'N, 57^o15'E$, a location where the trajectory of buoy 14800 displayed a cyclonic loop (remember that this buoy was drogued at 50m depth). Along the Iranian coast, cold and fresh water is found near $25^o15'N, 59^o15'E$ (under the cold coastal patch) and near $24^o40'N, 58^o30'E$ (under the detached cold blob). Figure 15b shows that the depth of this isopycnal varies between 70 and 130m. It domes

[10]Note that on the LADCP network, the currents presented here are those measured by the SADCP except at 800m depth

near the center of the Gulf of Oman.

Currents at 100 m depth also form a cyclonic loop between 24^oN and 25^oN and $58^o30'E$ and 60^oE. In the SADCP network (figure 15d), the circulation between 24^oN and $25^o30'N$ and 57^oE and 58^oE also appears cyclonic but not closed and with weaker currents. A small anticyclonic region is found near $25^oN, 58^o15'E$ near the detached cold blob. Currents along the Omani coast form a strong jet (with $0.3m/s$ velocity near the Strait, and $0.5m/s$ near the opening of the Gulf of Oman); this jet widens east of Ra's al Hamra, as seen also in the LADCP network (Figure 15c). This LADCP network shows currents at the mouth of the Gulf of Oman and in the Arabian Sea nearly aligned with those at thermocline level.

4.3 Hydrology and circulation at the level of the PGW core

At the level of the PGW core, the lateral thermohaline front between PGW and neighboring waters clearly appears in the salinity map on isopycnal surface $\sigma_0 = 26.5$ (Figure 16a). The PGW outflow heads southeastward on the shelf down to $25^o15'N, 57^o15'E$, then veers southwestward and joints the Omani coast downstream. This coastal current undergoes meandering; a cold cyclonic meander lies near $24^o30'N, 57^oE$, below the cyclonic loop of buoy 14800; it is followed by an anticyclonic one upstream of Ra's al Hamra (see 3.2). PGW has slightly weaker salinity at the mouth of the Gulf of Oman than in the northern Arabian Sea. Near the Iranian coast (near $24^o40'N, 58^o20'E$), cold and fresh water ($17^oC, 36.25$ psu) is found under the detached blob of upwelled waters at the thermocline and IOSW levels (see the previous two subsections). Elsewhere along the Iranian coast lies essentially cold and fresh water (with minimum $T = 17.5^oC$ and $S = 36.5$ psu).
Figure 16b shows the depth of isopycnal $\sigma_0 = 26.5$; it is shallow near the Strait (roughly 140m) and the deepest along the eastern coast of Iran (270m). In general, it is deeper near the coasts (between 220 and 250m) and shallower at the center of the Gulf of Oman (160m).

Currents at PGW level resemble those at shallower levels, with a thin jet along the Omani coast (with velocity on the order of $0.2m/s$). Downstream of Ra's al Hamra, velocity maximum (on the order of $0.4m/s$) lies offshore and comes back to the coast at the mouth of the Gulf of Oman (LADCP network, figure 16d). In the SADCP network (figure 16c) the velocity maximum is more spread out offshore, downstream of Ra's al Hamra (as if the coastal flow merged with regional circulation). In the SADCP network again, anticyclonic rotation is observed in the region of cold and fresh water near the Iranian coast (near $25^oN, 58^oE$). The regional circulation is a clear cyclonic gyre between 24^oN and 25^oN, $58^o30'E$ and 60^oE. The currents in the western part of the Gulf of Oman (near the continental shelf) are also cyclonic, but do not close as a gyre. The SADCP network (Figure 16c) evidences northeastward currents near the Iranian coast at the mouth of the Gulf of Oman. Currents at this depth and location exit from the Gulf of Oman. Finally, currents in the northern Arabian Sea are southward near 60^oE and northward near 61^oE.

Figure 8b summarizes these observations by showing the vertical section of density on S01 (from $(23^o10'N, 59^o10'E$ to $25^oN, 60^oE)$. Isopycnals below $\sigma_\theta = 25$ form a dome (except close to the Omani coast with the PGW core) in relation with the baroclinic cyclonic circulation down to 300 m depth.

4.4 Deeper water masses and flow

The isopycnal $\sigma_0 = 27.35$, at depths ranging between 750 and 900m, is chosen as representative of the level of Red Sea Water (figure 17b). At that level, temperature and salinity data are more scarce and the resulting map is patchy (Figures 17a). Traces of warm and salty water ($10.3^oC, 35.55$ psu) are found along the Omani coast under the PGW core. Colder and fresher water ($10.2^oC, 35.52$ psu) occupies the central/eastern part of the Gulf of Oman (near $24^oN, 60^oE$) and is much shallower than surrounding waters. A patch of warm and salty water ($10.5^oC, 35.6$ psu) is found 100km offshore of the Ira-

nian coast. In the Arabian Sea, the water is warm and salty RSW ($10.5^oC, 35.56$ psu) in particular near $21^o30'N, 60^oE$. The few velocity measurements at such depths (only reached by LADCP) reveal eastward currents along the Omani coast (with peaks at $0.2m/s$) and provide a sketchy indication of cyclonic motion at basin scale in the western Gulf of Oman (Figure 17c).

5 Summary and conclusions

Data analysis of GOGP99 experiment has clearly shown the southeastward outflow of PGW from the Strait of Hormuz, flowing on the seabed. It then crosses the shelfbreak, veers southwestward and joins the Omani coast (in fact the 200m isobath) to form a slope current near 200-250 m depth (centered on isopycnal $\sigma_0 = 26.5$); this currents then progresses southeastward along the Omani coast at $0.2m/s$, and faster downstream of Ra's al Hamra (see figure 18a). This current veers around Ra's al Hadd and enters the Arabian Sea, where it lies offshore (see figure 18b). The Ra's al Hadd front is thus not a permanent obstacle to PGW intrusion into the Arabian Sea.

Everywhere along its path, the PGW core maintains a sharp thermohaline difference with the surrounding water masses, allowing its identification. But these thermohaline characteristics of the PGW core decrease from $27^oC, 39.75$ psu in the Gulf to $T = 21^oC, S = 37.1$ psu in the northern Arabian Sea. This decrease is not uniform though, and PGW intensely mixes with the neighboring water masses at a few locations: in the Strait of Hormuz, turbulent mixing of PGW with IOSW can result from varying wind-stress and bottom friction; at shelfbreak, breaking internal waves and PGW cascade can create turbulent mixing with the colder and fresher water at 100-200m depths, though no direct measurement of finescale structure was performed to confirm these mechanisms. Farther downstream, mixing is likely to result from mesoscale variability. The temperature drop at shelfbreak is the largest along the path of PGW, in agreement with previous work by Bower et al. (2000) based on a streamtube model of the outflow.

Noticeable lateral spreading of the outflow is also observed at shelfbreak, as the PGW outflow cascades down the slope; then, the current widens and forms a meander upstream of Ra's al Hamra (see again figure 18a). This meander can amplify under the influence of baroclinic instability of the PGW current. A simple (three-layer) quasi-geostrophic model was used to quantify the most unstable wavelengths and their growth rates in this case (despite the steep bottom slope). It provided results (approx. 100km) in agreement with observations. This instability could be triggered by a local irregularity of isobaths. This meander could also be due to time variability of the PGW outflow (and the cyclone upstream from vortex stretching at shelfbreak). Indeed, the successive hydrological networks show a variability of about 15-20 day period in the evolution of temperature and salinity maxima, from the Strait to the mouth of the Gulf of Oman. The stationarity of the meander upstream of Ra's al Hamra (already observed by Bower et al., 2000) may be due to the presence of the cape or to a vorticity image at the coast. Downstream of Ra's al Hamra, the velocity maximum of the PGW outflow lies offshore and anticyclonic shear is observed inshore as described by theory and laboratory experiments of flow encountering a cape (in a stratified fluid) and developing anticyclonic recirculation in its lee.

The PGW current progresses southeastward along the Omani coast at $0.2m/s$ on average with local maxima at $0.5m/s$. In fact, ADCP measurements near the Omani coast indicate that all water masses in the upper 300 meters flow southeastward. The regional circulation at the center of the Gulf of Oman is a cyclonic gyre between 24^oN and 25^oN and between $58^o30'E$ and 60^oE (see figure 19). This circulation is clearly visible in the upper 300 meters. The circulation in the western end of the Gulf of Oman is also cyclonic but is not closed (and therefore does not constitute a gyre *per se*). An anticyclonic region of cold and fresh water lies along the Iranian coast near $25^o15'N, 59^oE$. This patch with characteristics of an upwelling is intensified

during the second half of October. The westward currents along the Iranian coast are associated in the upper 200 m with advection of cold water. Both this upwelling and this advection of cold water can be correlated with the increase of IOSW near the Strait of Hormuz, mentioned in Part 1 of the paper. Finally note the existence of a deep outward flow at the opening of the Gulf of Oman.

Though the data allowed a description of the PGW core and of the regional circulation, it did not solve (by far) all questions asked in this paper. Further work should include:
- establishing more accurately the correlation between this regional circulation and the general circulation in the Arabian Sea or with the wind regime and orographic effects in the Gulf of Oman;
- determining the longer time-scale variability of the PGW outflow and of the regional circulation in response to external forcings (atmospheric fluxes, formation of PGW in the Gulf, large and mesoscale dynamics of the Arabian Sea);
- investigating the existence of a permanent outflow of warm and salty surface water from the Gulf into the Gulf of Oman (and along the Omani coast);
- performing a detailed study of meanders and eddies of PGW (analysis of the transport and potential vorticity upstream of these meanders, analysis of the structure and formation sites of meanders and eddies, of their decay rate and mechanisms, vortex census in the Gulf of Oman over at least a year);
- clearly identifying the upwelling events near Ra's Jagin (Iranian coast) and their variability;
- describing completely (over the long run) the penetration of PGW into the Arabian Sea (and its propagation southwards).
Answering these questions imply long-term measurements in the Gulf and along the Omani and Iranian coasts with thermistor and ADCP moorings, the availability of accurate and high resolution winds and atmospheric fluxes, repeated hydrological surveys at various seasons of a given year and periodic release of subsurface acoustic floats (a similar effort to that recently made in the Gulf of Cadiz). Considering the cost of such an intensive (and extensive) experimental array, high-resolution modeling of this Gulf could bring complementary information on the dynamical processes governing the evolution of the PGW core and of the regional circulation.

acknowledgments

It is a pleasure to thank Yves Camus and Eric Duporte (SHOM/CMO/CM) for their essential participation in the design of the GOGP99 experiment. Captains and Crews of R/V D'Entrecasteaux and Laplace played an essential role in data collection; EPSHOM/CMO/CM engineers and technicians participated in data processing. Dr Abderrahim Bentamy (LOS, IFREMER) kindly provided the daily winds over the Gulf of Oman, from the CERSAT database; we gratefully acknowledge his help. This work is a contribution to the GOGP99 program and to S. Pous Ph.D. thesis.

Appendix : dynamical analysis of the origin of the PGW meander

Baroclinic instability of the PGW current

The presence of a cyclonic motion upstream and above the anticyclonic meander of PGW, upstream of Ra's al Hamra suggests that baroclinic instability may be a mechanism underlying the growth of this meander. Therefore, an analytical three-layer quasi-geostrophic model is used to quantify baroclinic instability of the PGW core locally. This three-layer model is an extension of the Phillips model (1954), with linear dynamics and horizontally uniform flow. It has been widely described by Smeed (1988) and by Pichevin (1998).

To calibrate this model, we first examine the local stratification on section R07. The first three baroclinic modes and their corresponding radii of deformation are computed at four stations of this section (see figure 10 and table 3). Clearly, at stations 412 and 413, the second baroclinic mode is intensified at the depth of the PGW core which is sampled by these two stations. They indicate that the appropriate deformation radii should be close to 20-24km for the first internal radius, and to 12-14km for the second.

We set the stratification with the mean density $\rho_0 = 1025 kg/m^3$ and the two density jumps $\Delta\rho_1 =$

$1.2kg/m^3$, $\Delta\rho_2 = 0.8kg/m^3$. The layer thicknesses are chosen as $h_1 = 160m, h_2 = 120m, h_3 = 620m$ (based on station 412). This leads to internal deformation radii of 25km and 10.5km[11]. The Coriolis parameter is $f_0 = 6.4\ 10^{-5}s^{-1}$, its variations are neglected and the bottom slope is $\Sigma = -2.3\ 10^{-2}$. The reference frame is aligned with the isobaths and the coastline (assumed parallel here). Thus the mean flow is zonal in the model. SADCP sections at S05 (see figure 6e) and S07 indicates that the velocity in the upper 150m is close to $0.2-0.3m/s$ and decreases to $0.1-0.2m/s$ between 150 and 250m depths. Note that the PGW outflow *does not* correspond to a local velocity maximum along the vertical axis.

Here, we choose two sets of values for the layerwise velocities (U_1, U_2, U_3) : $(0.2, 0.15, 0.0)m/s$, $(0.3, 0.2, 0.0)m/s$ when considered over flat bottom (cases fb-005-015, fb-01-03). We retain the last set of values when we add the bottom slope. Note that this slope is very steep : across the core width (30km), it results in a variation of topographic height equal to the lower layer thickness. Such a steep slope does not satisfy the quasi-geostrophic assumptions and caution must be exerted on the interpretation of this case.

Over flat bottom, the most unstable wavelengths are close to 110km, with corresponding growth rates varying between 1/20 and 1/10 day^{-1}, for the two cases having different vertical shears of the mean flow (see figure 11). The wavelength is comparable with the Bower et al. finding; it is also compatible with the upper bound provided by our sections. Concerning the growth rate, our data do not allow its experimental determination since the meander is rather in a separation stage from section R07 to section S05 (two weeks later).
Inserting the real bottom slope in this model does not susbtantially modify the growth rate (which remains close to 1/12 day^{-1}) but reduces the most unstable wavelength to 60km. Again accuracy of a quasi-geostrophic model under such conditions is questionable, and further work with a primitive equation model will be required to definitely solve this case. Still, the quasi-geostrophic model provides a realistic order of magnitude for the characteristics of the instability in the flat bottom case. Note that the most unstable wavelength is then 2π times a radius intermediate between Rd_1 and Rd_2 at stations 411 to 414. This suggests that the first two baroclinic modes play an essential role in this mechanism (under the strong hypotheses of the model).

[11] it has not been possible to obtain radii closer to observed values while retaining realistic values for layer thicknesses and density jumps

Influence of the time-variation of the transport of the PGW current

The meander of the PGW outflow could also be due to the time variation of its transport. In section 3.3, we have seen that variations of the outflow on a 15-20 day period are observed along its path. In 1991, D. Nof studied this mechanism to predict the splitting of a coastal current into $n > 1$ separate eddies. Since only one meander is observed here, this theory cannot be applied as it stands, but this mechanism could be called upon to explain the local accumulation of water in the meander. In this case, conservation of volume must be checked. The volume of the outflow during a $\Delta t = 15day$ period is $T\Delta t$, where T is the transport of PGW; this volume must be compared to the volume of a meander $H\pi R^2/2$ (idealized as a half-cylinder with an offshore extent half the wavelength). Here we have $H = 120m$, $R = 50km$.
The transport upstream of the meander is determined on section S07 with a PGW core width of $30km$, a thickness of $100m$ and an average velocity of $0.2m/s$, leading to $T \sim 0.6Sv$ (a value comparable to the 0.8-1.0 Sv found by Bower et al. beyond shelfbreak). The volumes are then $T\Delta t \sim 780km^3$ and $\pi HR^2/2 \sim 470km^3$. The local accumulation of PGW in a blob, due to the variation of the transport, is therefore possible.

Influence of bottom slope on the PGW current

Another mechanism for the formation of anticyclonic lenses from a slope current has recently been proposed by Nof et al. (2002). The authors state that the current will flow undisrupted if the

velocity distribution is one-signed (especially near the coast). Otherwise the current will form a chain of eddies. Under the assumption that the current is parallel, the authors determine the topographic and potential vorticity contributions to the mean velocity. The resulting condition for the current not to break is $g'S/f > \alpha\sqrt{g'H}$ where g' is the reduced gravity between the outflow and the surrounding waters, H is the maximum thickness of the outflow, S is the bottom slope and f is the Coriolis parameter. The parameter α depends on the potential vorticity distribution and, according to Nof et al., is of order unity. Here, we do not precisely know the potential vorticity distribution in PGW near the coast (because we lack high resolution hydrological and velocity data there). Therefore the previous formula is used here for a current with constant potential vorticity; in this case, the current will be stable if $g'S/f > \sqrt{g'H}$. The parameters are $S = 2.3\,10^{-2}$, $f = 6.4\,10^{-5}s^{-1}$, $g' = 10^{-2}m/s^2$, and $H = 120m$; the left-hand term of the formula is then equal to 3.6 and the right-hand one to 1.1. Under these assumptions, this mechanism cannot be held responsible for the formation of a PGW meander. But since α depends on the PGW potential vorticity, specific measurements should be made to determine it more precisely.

Location of the meander

Another question is why these meanders are observed nearly at the same location (see the Bower et al. 2000 data). If baroclinic instability is responsible for their growth, it could be triggered by a topographic spur. And indeed, the 200m isobath is indented offshore near $24^o25'N, 57^o10'E$[12]. If time variation of the PGW outflow is responsible for the formation of meanders, their local amplification could be favored by the presence of a cyclonic motion upstream. This cyclonic motion could result from the vortex stretching of the upper water column when the PGW outflow cascades down the continental slope. The cyclones would then form when the PGW outflow intensifies and subsequently they would participate in the breaking up of this outflow when it weakens. The absence of downstream propagation of this meander could be also due to the presence of the Ra's al Hamra cape downstream or to a wall image effect (this image being positive vorticity inside the coast, thus generating an upstream velocity against the mean flow).

[12] a similar effect was observed on the Mediterranean outflow southwest of Portugal; see the Surdrift buoy trajectories in Chérubin et al., 2000

References

[1] Admiralty Pilot, Persian Gulf and Gulf of Oman, Hydrographer of the Navy, London, U.K., 1982.

[2] Banse K., Irregular flow of Persian(Arabian) Gulf water to the Arabian Sea, *J. Mar. Res.*, 55(6), 1049-1067, 1997.

[3] Bower A.S., H.D. Hunt and J.F. Price, Character and dynamics of the Red Sea and Persian Gulf outflows, *J. Geophys. Res.*, 105(C3), 6387-6414, 2000.

[4] Bower D.L. and L. Tao, On the motion of linearly stratified rotating fluids past capes, *J. Fluid Mech.*, 180, 429-229, 1987.

[5] Cagle B.T. and R. Writner, Arabian Sea project of 1980 - composites of infrared images, Office of Naval Research ONRWEST 81-5, 16pp, 1981. 1030 East Green Street, Pasadena, Ca. 91106 USA.

[6] Chérubin L.M., Carton X., Paillet J., Morel Y. and A. Serpette, Instability of the Mediterranean water undercurrents southwest of Portugal: effects of baroclinicity and of topography, *Oceanologica Acta*, 23, 551-573, 2000.

[7] Davies P.A., Besley P. and D.L. Boyer, An experimental study of flow past a triangular cape in a linearly stratified fluid, *Dyn. Atmos. oceans*, 14, 497-528, 1990.

[8] Flagg C.N. and H.S. Kim, Upper ocean currents in the northern Arabian Sea from ship board ADCP measurements collected during the 1994-1996 U.S. JGOFS and ONR programs, *Deep-Sea Res. Part II*, 45, 1917-1959, 1998.

[9] Johns W.E., F. Yao, D.B. Olson, S.A. Josey, J.P. Grist and D.A. Smeed, Observations of seasonal exchange through the Straits of Hormuz and the inferred heat and freshwater budgets of the Persian Gulf. *J. Geophys. Res.*, 108, C12, 3391, doi:10.1029/2003JC001881, 2003.

[10] Matsuyama M., Y. Kitade, T. Senjyu, Y. Koike and T. Ishimaru, Vertical structure of a current and density front in the Strait of Hormuz, in it Offshore Environment of the ROPME Sea Area after the war-related oil spill, edited by A. Otsuki, M.Y. Abdulraheem and R.M. Reynolds, Terra Sci. Publ. Co., Tokyo, 23-34, 1998.

[11] Nof D., Lenses generated by intermittent currents. *Deep-Sea Res.*, 38, 325-345, 1991.

[12] Nof D., Paldor N. and S. Van Gorder, The Reddy Maker. *Deep-Sea Res.*, 49, 1531-1549, 2002.

[13] Phillips N.A., Energy transformations and meridional circulations associated with simple baroclinic waves. *Tellus*, 6, 273-286, 1954.

[14] Pichevin T., Baroclinic instability in a three-layer flow: a wave approach. *Dyn. Atmos. Oceans*, 28, 179-204, 1998.

[15] Prasad T.G., M. Ikeda and S.P. Kumar, Seasonal spreading of the Persian Gulf Water mass in the Arabian sea, *J. Geophys. Res.*, 106(C8), 17,059-17,071, 2001.

[16] Premchand K., J.S. Sastry and C.S. Murty, Watermass structure in the western Indian Ocean - Part II: the spreading and transformation of the Persian Gulf Water, *Mausam*, 37 , 179-186, 1986.

[17] Quraishee G.S., Circulation in the North Arabian Sea at Murray Ridge during S.W. monsoon, *Deep-Sea Res.*, 31(6-8A), 651-664, 1984.

[18] Reynolds R.M., Physical Oceanography of the Gulf, Strait of Hormuz, and the Gulf of Oman-Results from the Mt Mitchell Expedition, *Mar Pollution Bull.*, 27, 35-59, 1993.

[19] Rochford, D.J., Salinity maxima in the upper 1000 metres of the north Indian Ocean, *J. Mar. Freshwater Res.*, 15, 1-24, 1964.

[20] Roe H.S. J. et al., RRS Charles Darwin Cruise 104 Leg 1, 12 Feb - 19 Mar 1997. Sche herezade: an interdisciplinary study of the Gulf of Oman, Strait of Hormuz and the southern Arabian Gulf, *Southampton Oceanography Centre, Cruise Report No. 9*, 77 pp, 1997.

[21] Serra N. and I. Ambar, Eddy generation in the Mediterranean undercurrent. *Deep-Sea Res. II*, **49**, 4207-4223, 2002.

[22] Schlitzer R., Ocean Data View, http:\\www.awi-bremerhaven.de/GEO/ODV, 2003.

[23] Smeed D., Baroclinic instability of three-layer flows. Part 1. *J. Fluid Mech.*, 194, 217-231, 1988.

[24] Sultan S.A.R. and F. Ahmad, Surface and Oceanic heat fluxes in the Gulf of Oman. *Continental Shelf Res.*, 13(10), 1103-1110, 1993.

[25] Swift S.A. and A.S. Bower, Formation and circulation of dense water in the Persian Gulf, *J. Geophys. Res.*, 108(C1), 2003. doi:10.1029/2002JC001360.

[26] Tchernia P., Océanographie Régionale. *ENSTA*, 257 pp, 1978.

Table 1: Physical oceanography measurements taken during the GOGP1999 cruise

Section Name	Number of profiles	Data Type	Start Date	End Date
		Gulf of Oman Sections		
R09	10	CTD/LADCP	Oct. 08, 1999 05h46	Oct. 08, 1999 16h59
R07	29	CTD/LADCP, XBT, XCTD	Oct. 09, 1999 22h09	Oct. 11, 1999 12h59
R05	23	CTD/LADCP, XBT, XCTD	Oct. 11, 1999 18h21	Oct. 13, 1999 12h10
R18a	14	CTD, XBT, XCTD	Oct. 13, 1999 02h01	Oct. 13, 1999 10h11
R02	37	CTD/LADCP, XBT, XCTD	Oct. 13, 1999 22h56	Oct. 16, 1999 00h45
R04	18	CTD/LADCP	Oct. 16, 1999 17h27	Oct. 17, 1999 15h16
S07		SEASOAR	Oct. 21, 1999 15h18	Oct. 21, 1999 23h35
S09		SEASOAR	Oct. 22, 1999 19h54	Oct. 23, 1999 05h08
S08		SEASOAR	Oct. 23, 1999 05h33	Oct. 23, 1999 14h04
S06		SEASOAR	Oct. 23, 1999 14h42	Oct. 23, 1999 21h33
R18b	10	CTD	Oct. 23, 1999 05h44	Oct. 23, 1999 11h33
R22	14	CTD	Oct. 24, 1999 09h03	Oct. 25, 1999 17h01
A07	5	AXBT, AXCTD	Oct. 25, 1999 06h56	Oct. 25, 1999 07h34
A05	7	AXBT, AXCTD	Oct. 25, 1999 09h33	Oct. 25, 1999 11h14
A02	13	AXBT, AXCTD	Oct. 25, 1999 08h02	Oct. 25, 1999 08h55
R14	11	XBT, XCTD	Oct. 26, 1999 11h19	Oct. 26, 1999 15h00
R17	12	CTD	Oct. 29, 1999 10h52	Oct. 29, 1999 23h20
S05		SEASOAR	Oct. 29, 1999 06h42	Oct. 29, 1999 17h57
T01		SEASOAR	Oct. 29, 1999 18h22	Oct. 29, 1999 22h57
S03		SEASOAR	Oct. 29, 1999 23h24	Oct. 30, 1999 10h13
T02		SEASOAR	Oct. 30, 1999 10h39	Oct. 30, 1999 13h39
R16	9	CTD	Oct. 30, 1999 14h49	Oct. 30, 1999 22h28
S02		SEASOAR	Oct. 30, 1999 15h16	Oct. 31, 1999 04h57
R15	8	CTD	Oct. 31, 1999 10h38	Oct. 31, 1999 17h32
S01		SEASOAR	Oct. 31, 1999 09h49	Nov. 01, 1999 04h14
S12		SEASOAR	Nov. 01, 1999 04h26	Nov. 01, 1999 11h01
S11		SEASOAR	Nov. 01, 1999 11h06	Nov. 01, 1999 20h35
R18c	9	CTD	Nov. 01, 1999 08h40	Nov. 01, 1999 13h58
R19	5	CTD	Nov. 01, 1999 16h31	Nov. 01, 1999 19h07
R21	12	XBT	Nov. 02, 1999 11h39	Nov. 02, 1999 14h01
R01	32	CTD/LADCP, XBT, XCTD	Nov. 10, 1999 22h33	Nov. 12, 1999 00h39

Table 2: Distance of sections used in this paper from section R13, the closest one to PGW source

Section Name	Distance from R13
R13	0 km
R12	75 km
R11	125 km
R19	150 km
R18	195 km
R17	230 km
R16	300 km
R15/S07	335 km
R14/R07/S06	425 km
R05/S03	505 km
R04/S01	550 km
R02	700 km
R01	920 km

Table 3: First three baroclinic radii of deformation at four stations of section R07

Station	Local depth	Rd_1	Rd_2	Rd_3
414	500m	14km	9km	7km
413	900m	20km	12.5km	7.5km
412	1400m	24km	14km	10km
411	1850m	38km	17km	10km

Table 4: Surdrift drifters deployed during the GOGP1999 cruise

Buoy Name	Drogue Depth	Deployment			End Date	T	ΔL	V
		Start Date	Lat	Lon				
14677	15 m	Oct. 08, 1999	25^o59.94N	56^o54.24E	Nov. 06, 1999	30	679	20
14697	15 m	Oct. 09, 1999	25^o31.68N	57^o26.88E	Oct. 27, 1999	18	337	14
14800	50 m	Oct. 08, 1999	25^o02.04N	57^o21.84E	Nov. 12, 1999	35	952	31
14824	230 m	Oct. 10, 1999	25^o05.82N	57^o56.88E	Nov. 03, 1999	25	300	13
14979	85 m	Oct. 17, 1999	25^o55.26N	56^o31.68E	Nov. 08, 1999	23	304	12
14932	230 m	Oct. 30, 1999	25^o19.56N	57^o14.16E	Nov. 04, 1999	05	075	15

[13]T is the total operating time (day). ΔL = total displacement (km). V = Mean scalar speed (cm s^{-1}) of the low-pass filtered (at three days) Surdrift trajectories.

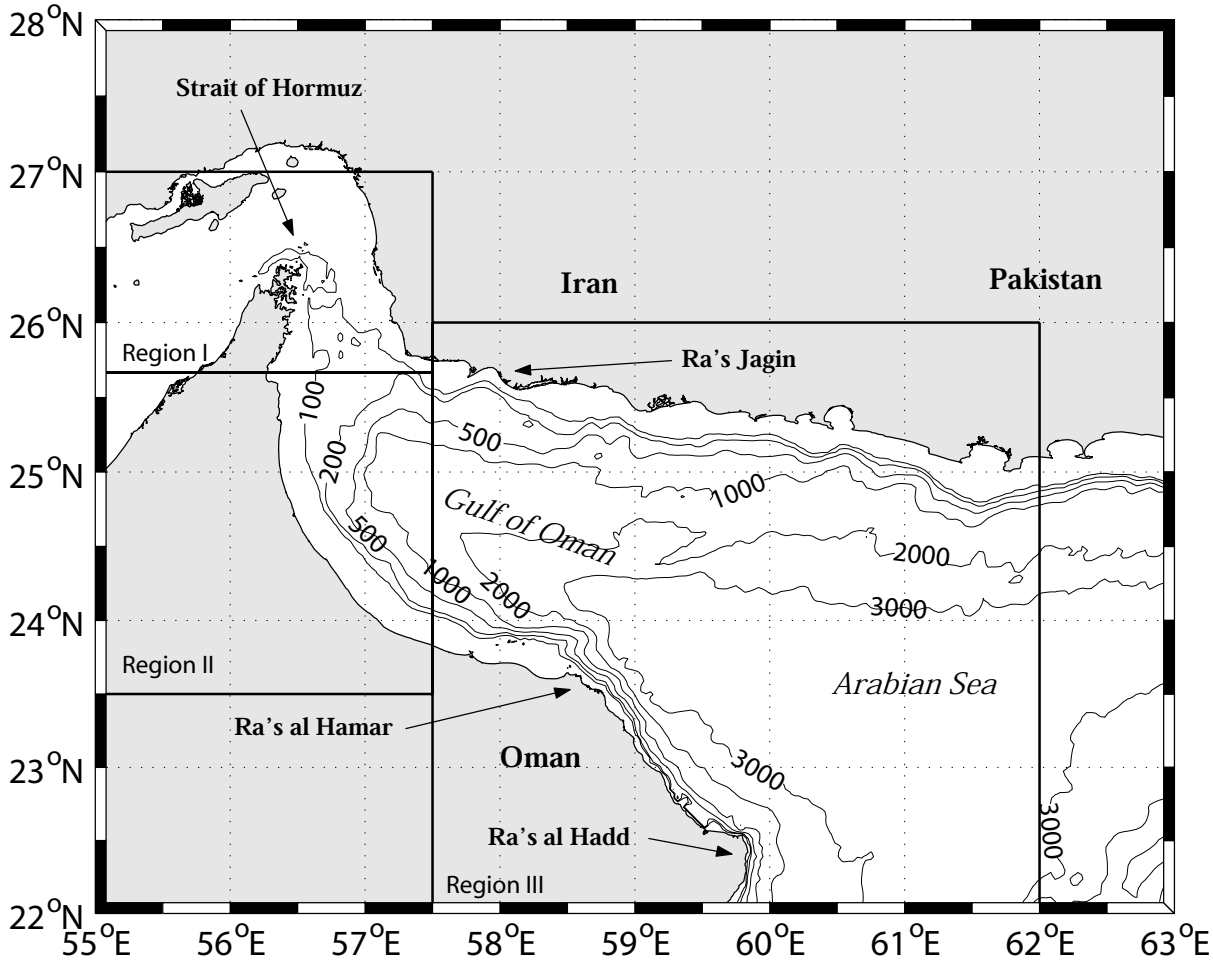

Figure 1: Geographic and bathymetric map of the Gulf of Oman and northern Arabian Sea. Isobaths from ETOPO2.

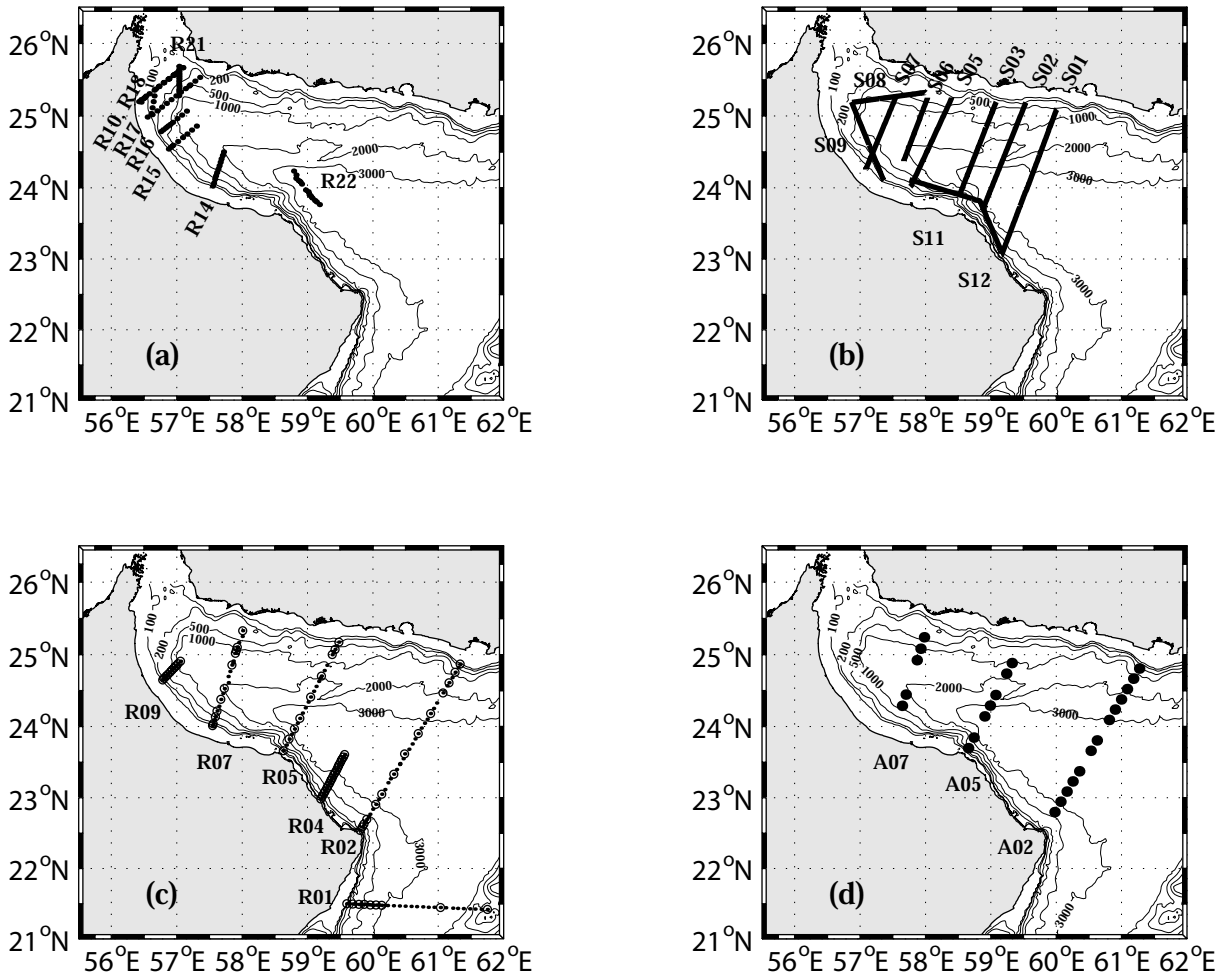

Figure 2: Maps of surveys achieved during GOGP99: (a) CTD stations, XBT and XCTD casts, (b) Seasoar transects, (c) CTD (dot)/LADCP (circle) stations, (d) AXBT/AXCTD casts.

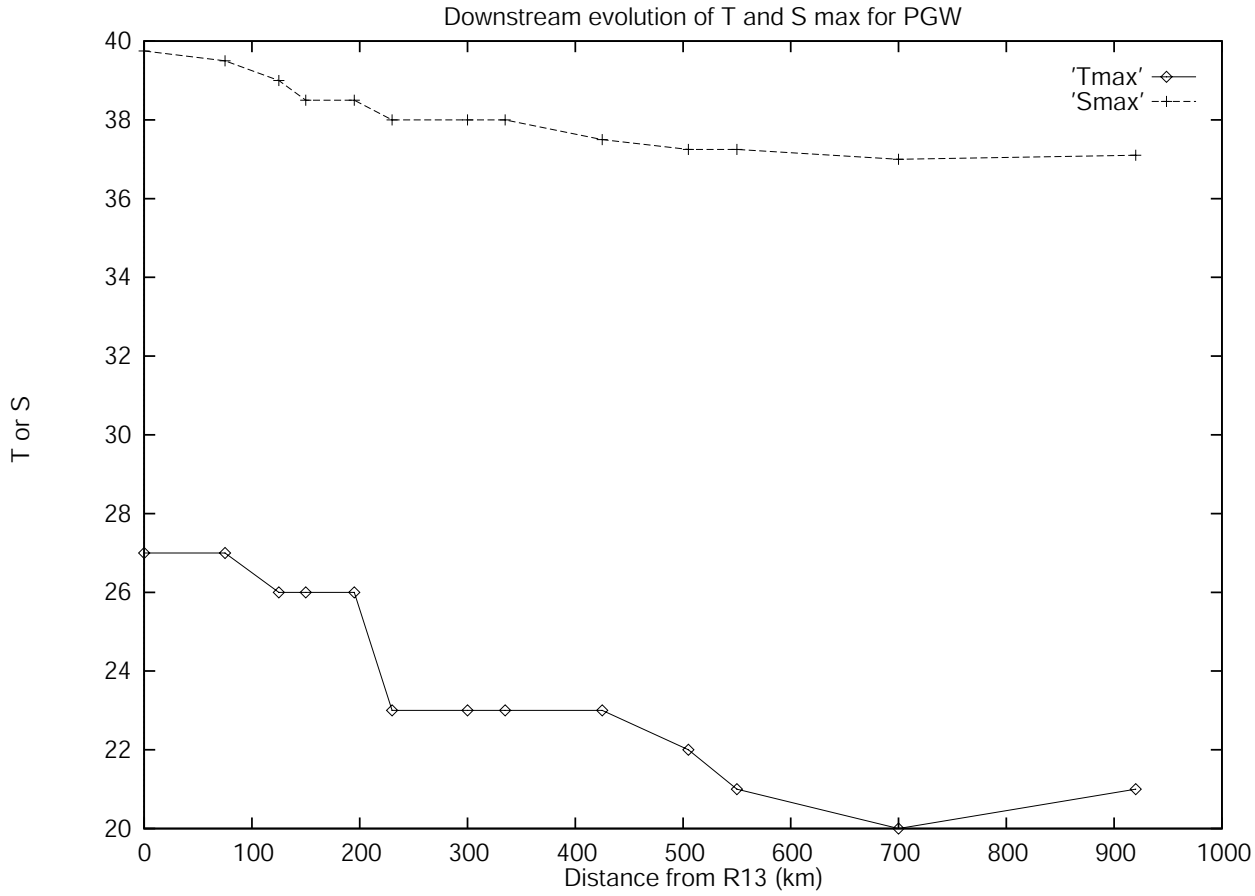

Figure 3: Evolution of temperature and salinity maxima for PGW from source (section R13 in the Gulf) to the Arabian Sea.

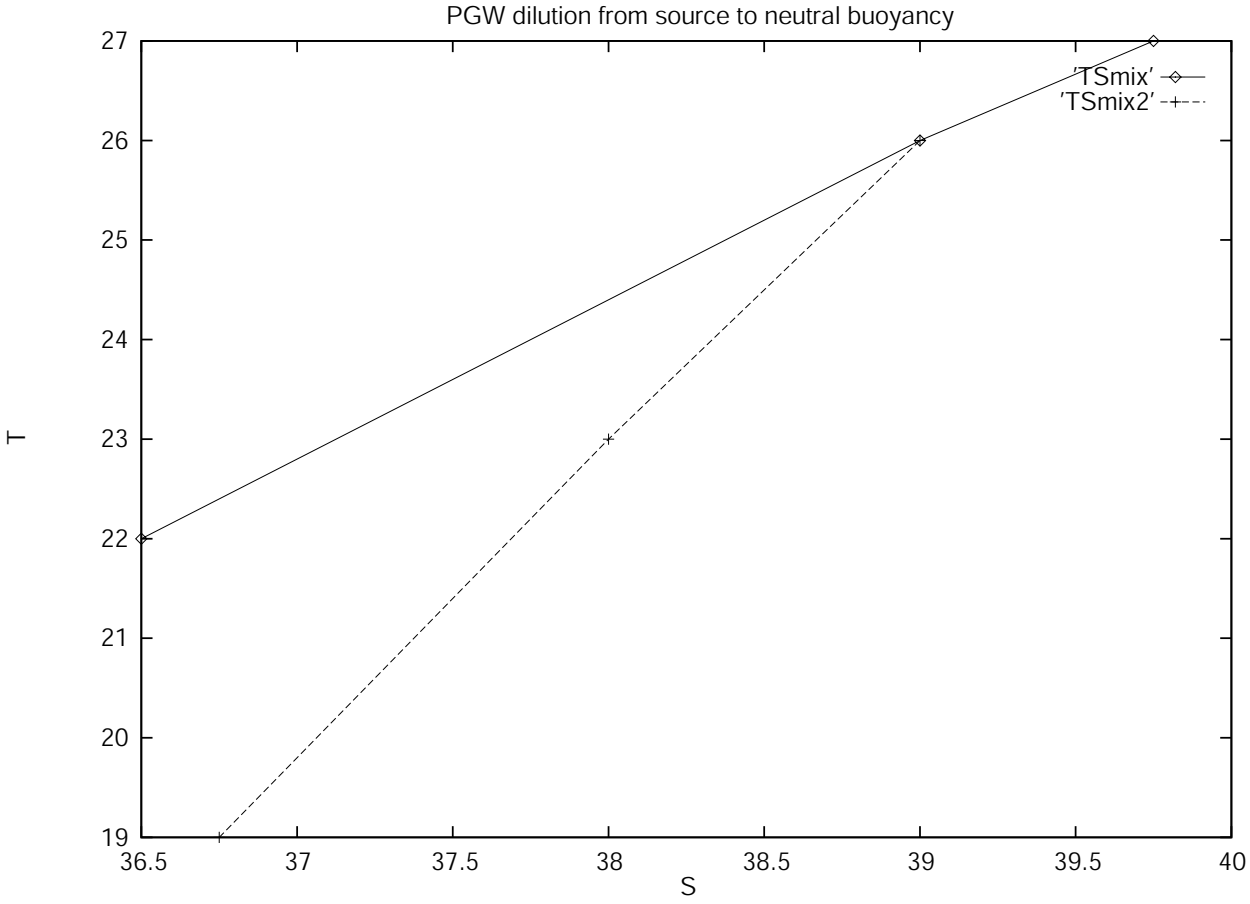

Figure 4: Mixing lines for PGW. The two lines respectively join the source PGW in the Gulf to the IOSW via PGW at shelfbreak, and PGW at shelfbreak to water masses at 200m depth in the Gulf of Oman via PGW in this gulf

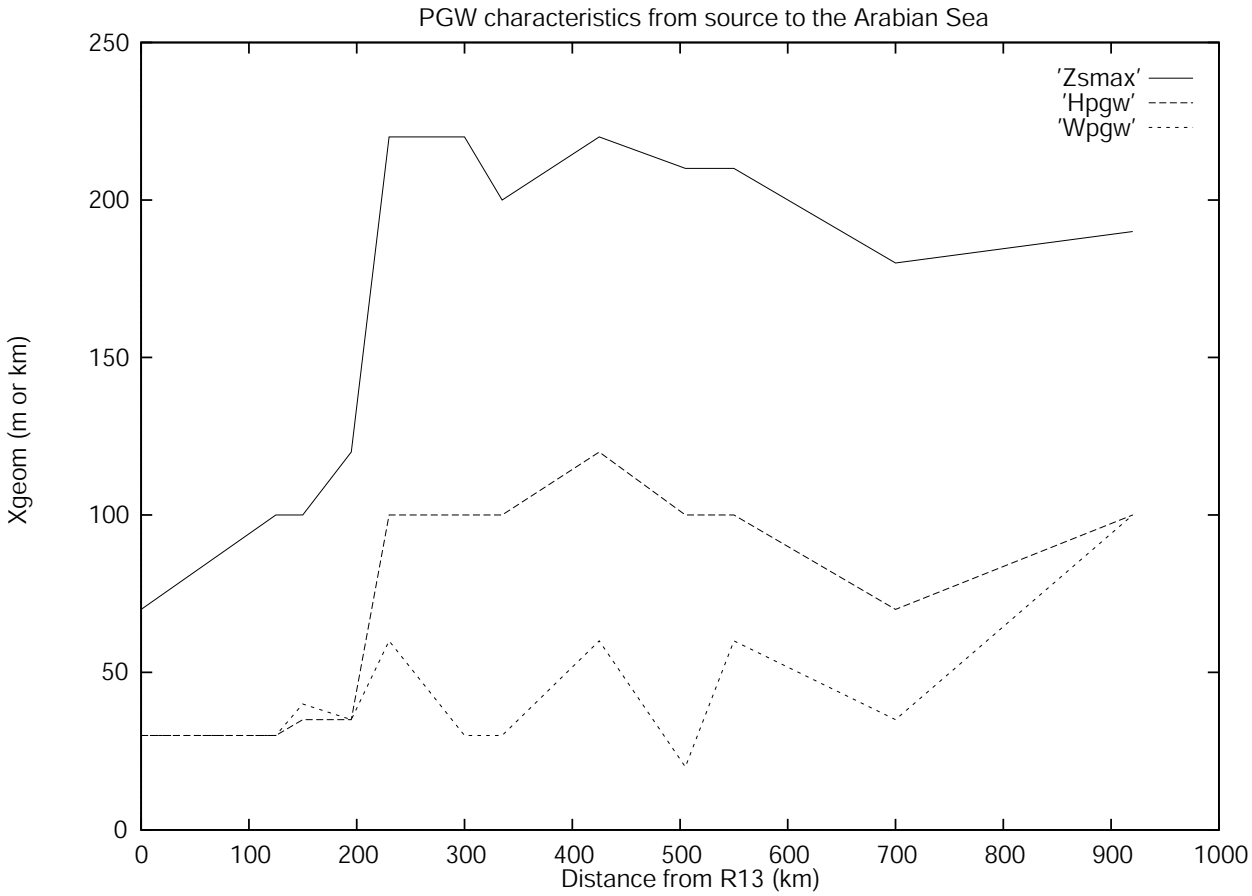

Figure 5: Evolution of the PGW depth, width and thickness from source to the Arabian Sea.

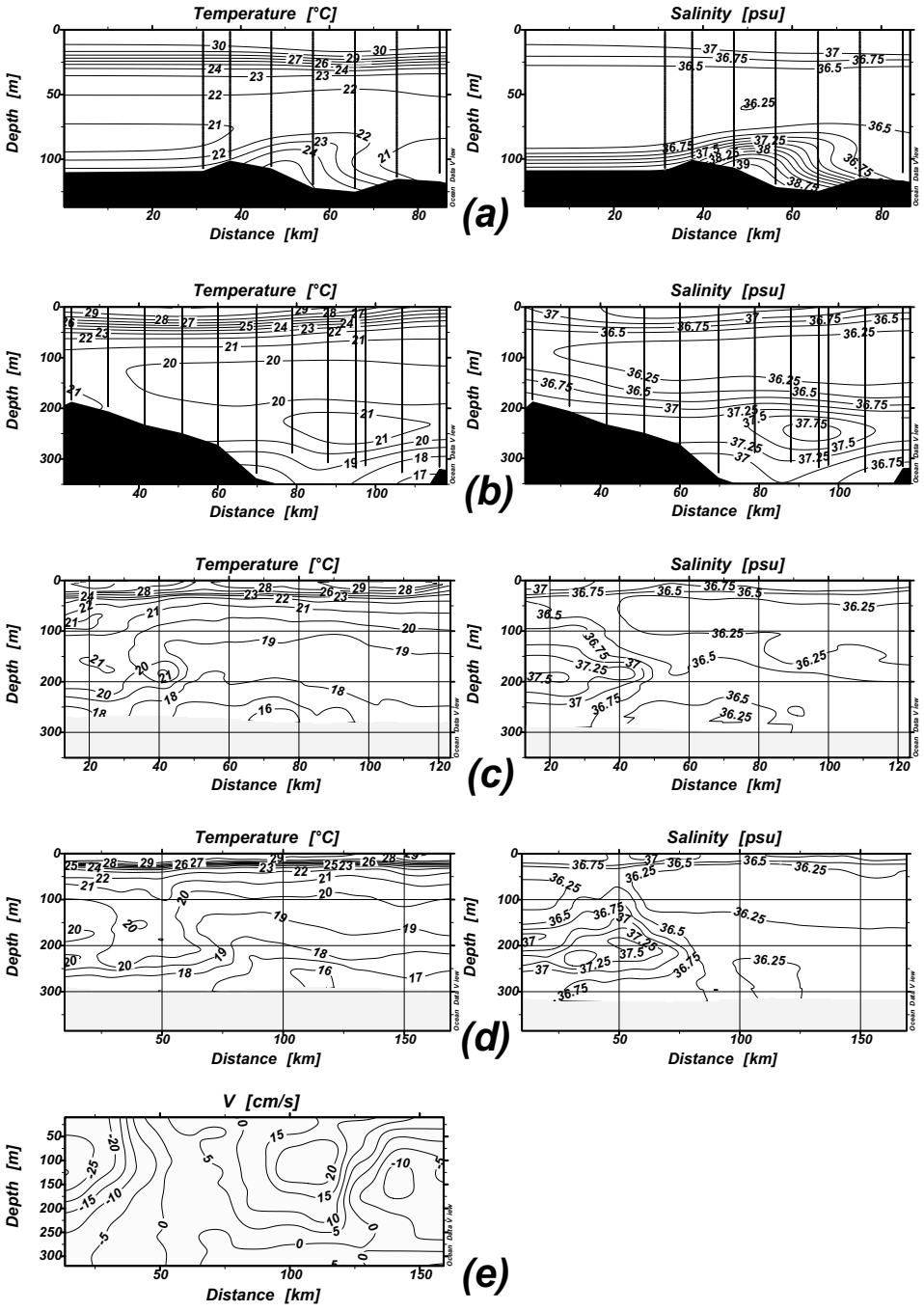

Figure 6: Vertical sections of temperature and salinity: (a) R18a, (b) R17, (c) S06, (d) S05 ; vertical sections of perpendicular velocity component from SADCP: (e) S05 (sections are drawn from the Omani coast to the Iranian waters, see figure 2 for location).

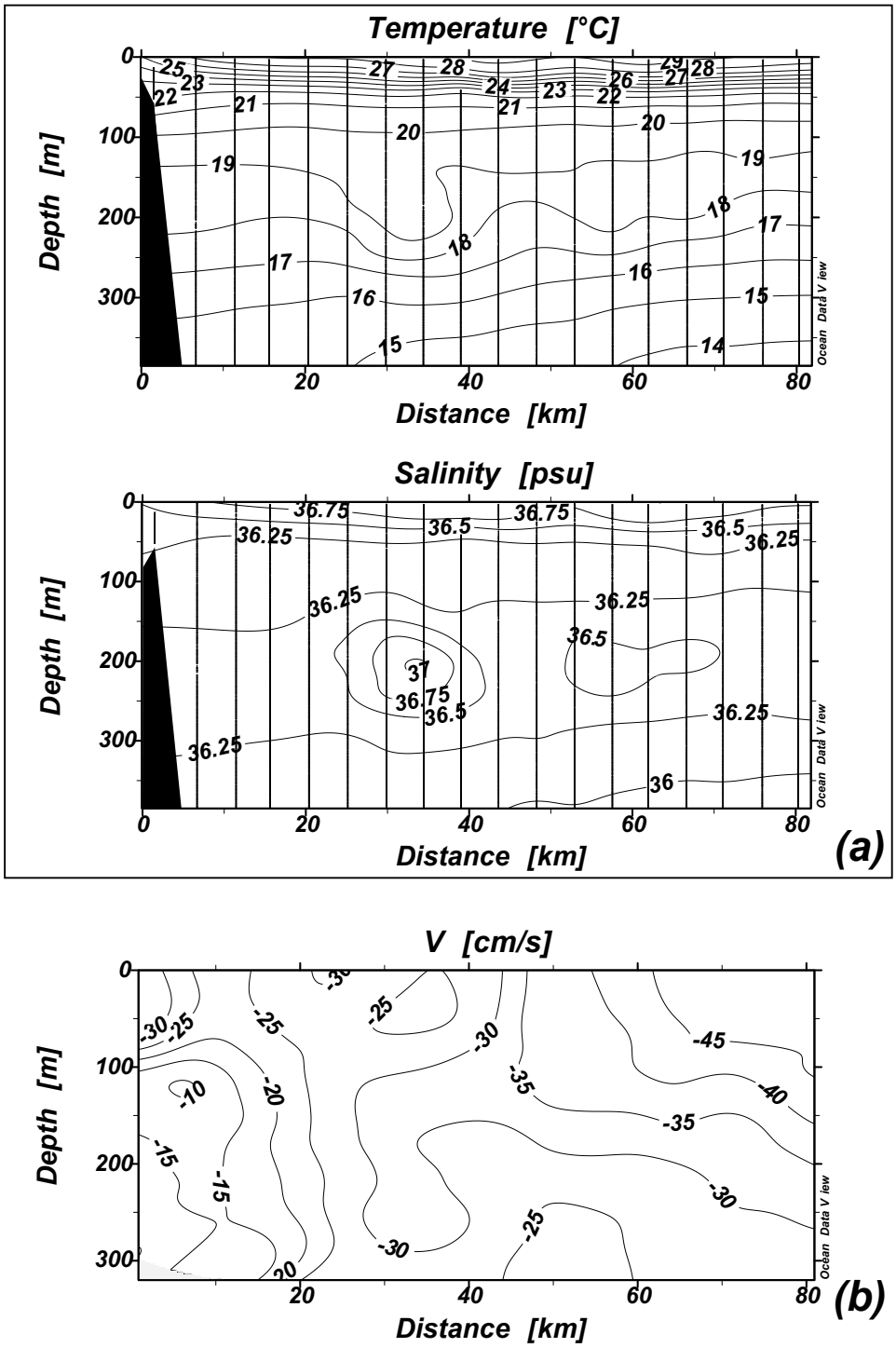

Figure 7: Vertical sections of temperature and salinity (a) and vertical section of perpendicular velocity component from SADCP (b) along section R04 (sections are drawn from the Omani coast to the Iranian waters, see figure 2 for location).

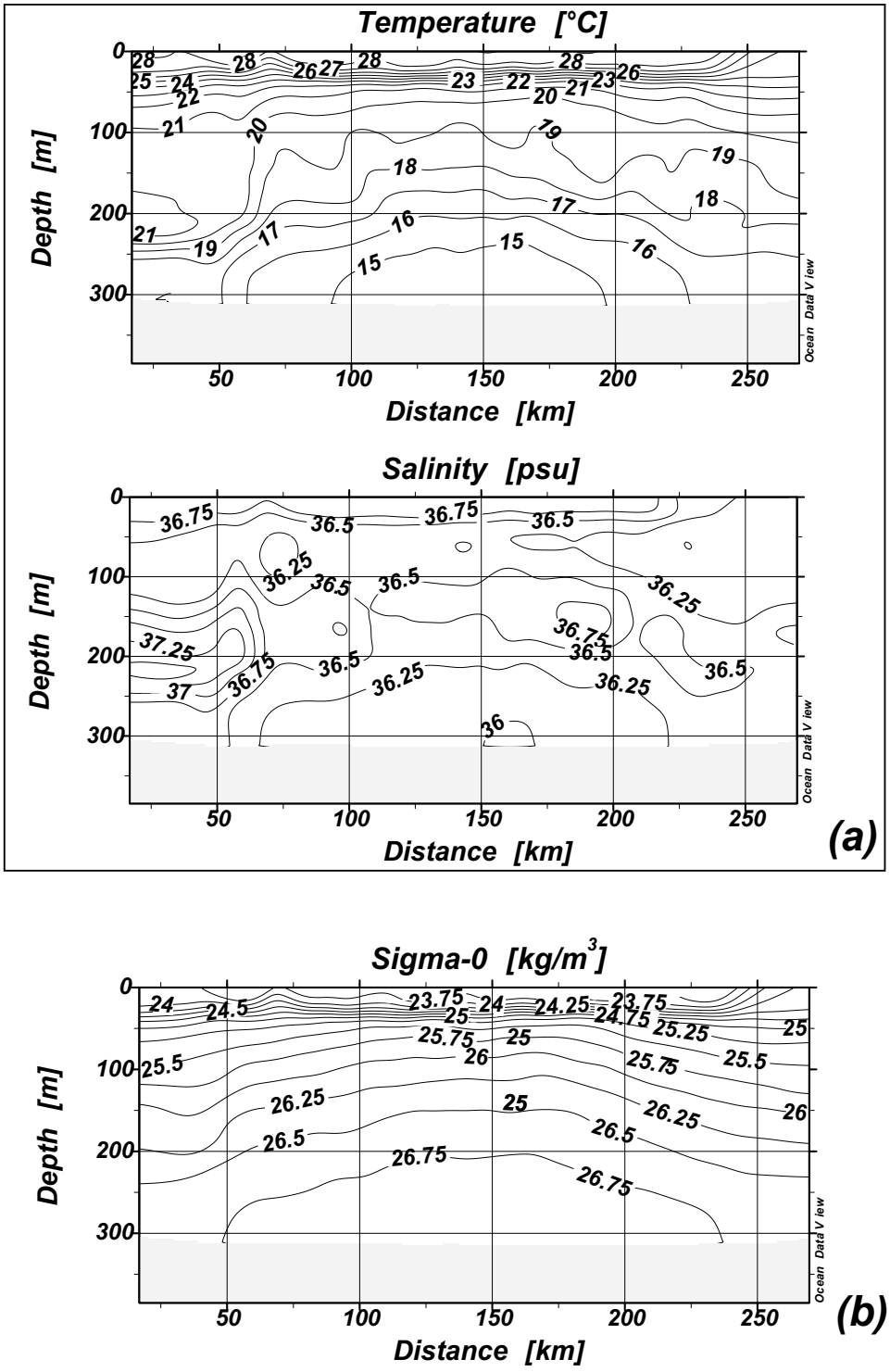

Figure 8: Vertical sections of temperature and salinity (a) and density (b) along section S01 (sections are drawn from the Omani coast to the Iranian waters, see figure 2 for location).

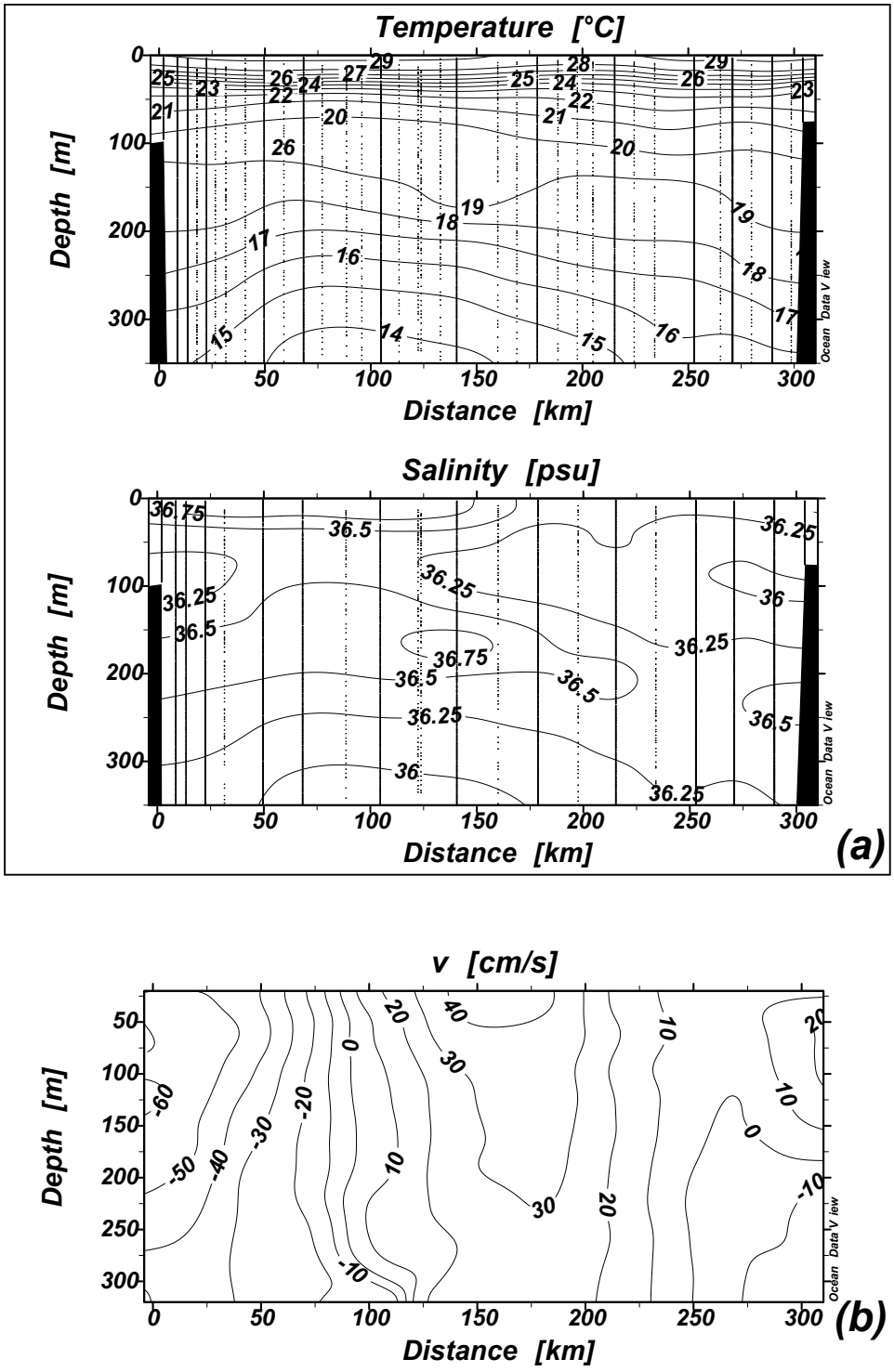

Figure 9: Vertical sections of temperature and salinity (a) and vertical section of perpendicular velocity component from SADCP (b) along section R02 (sections are drawn from the Omani coast to the Iranian waters, see figure 2 for location).

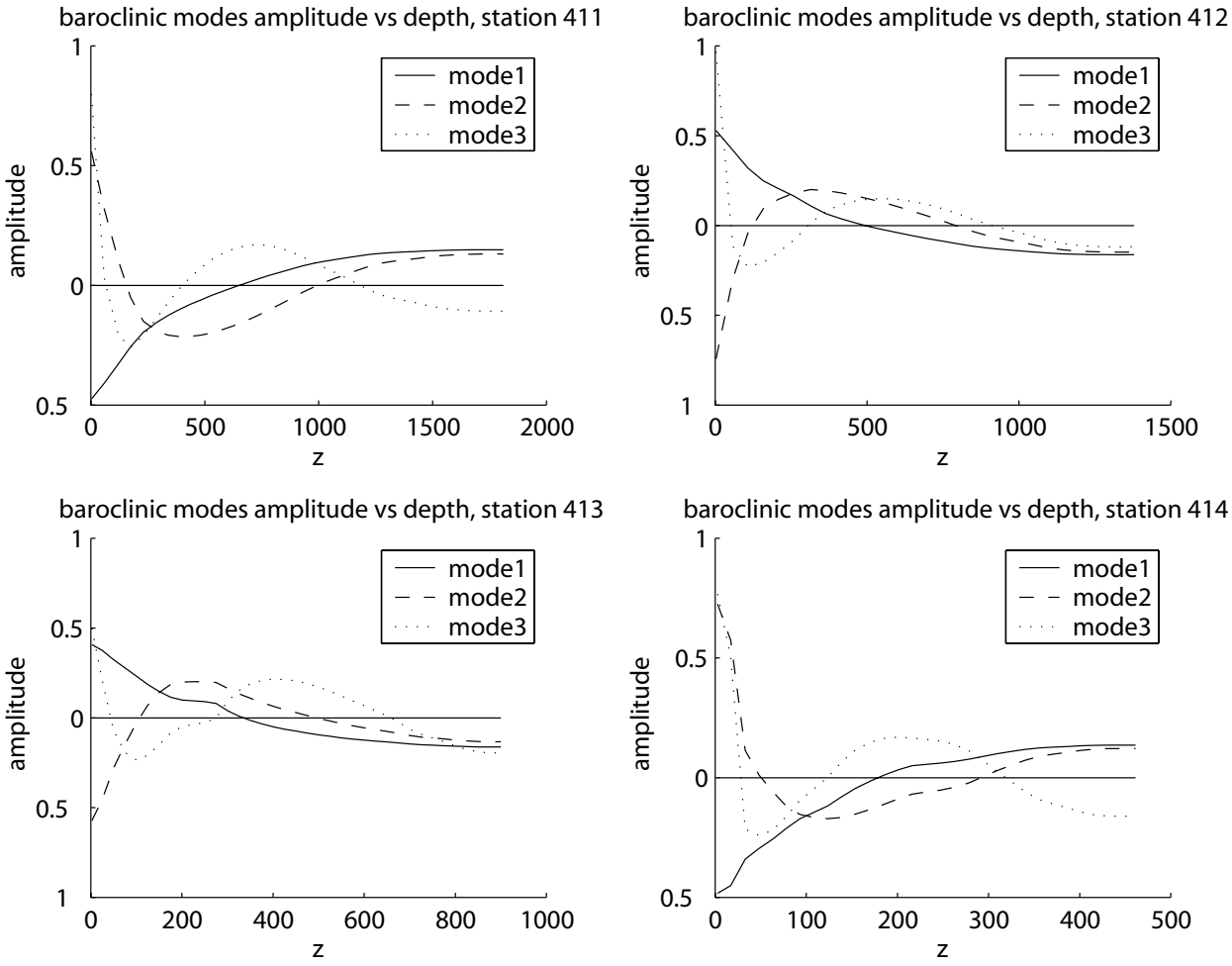

Figure 10: First three baroclinic modes for stations 411, 412, 413 and 414 (near Omani coast) on section R07 (see figure 2 for location).

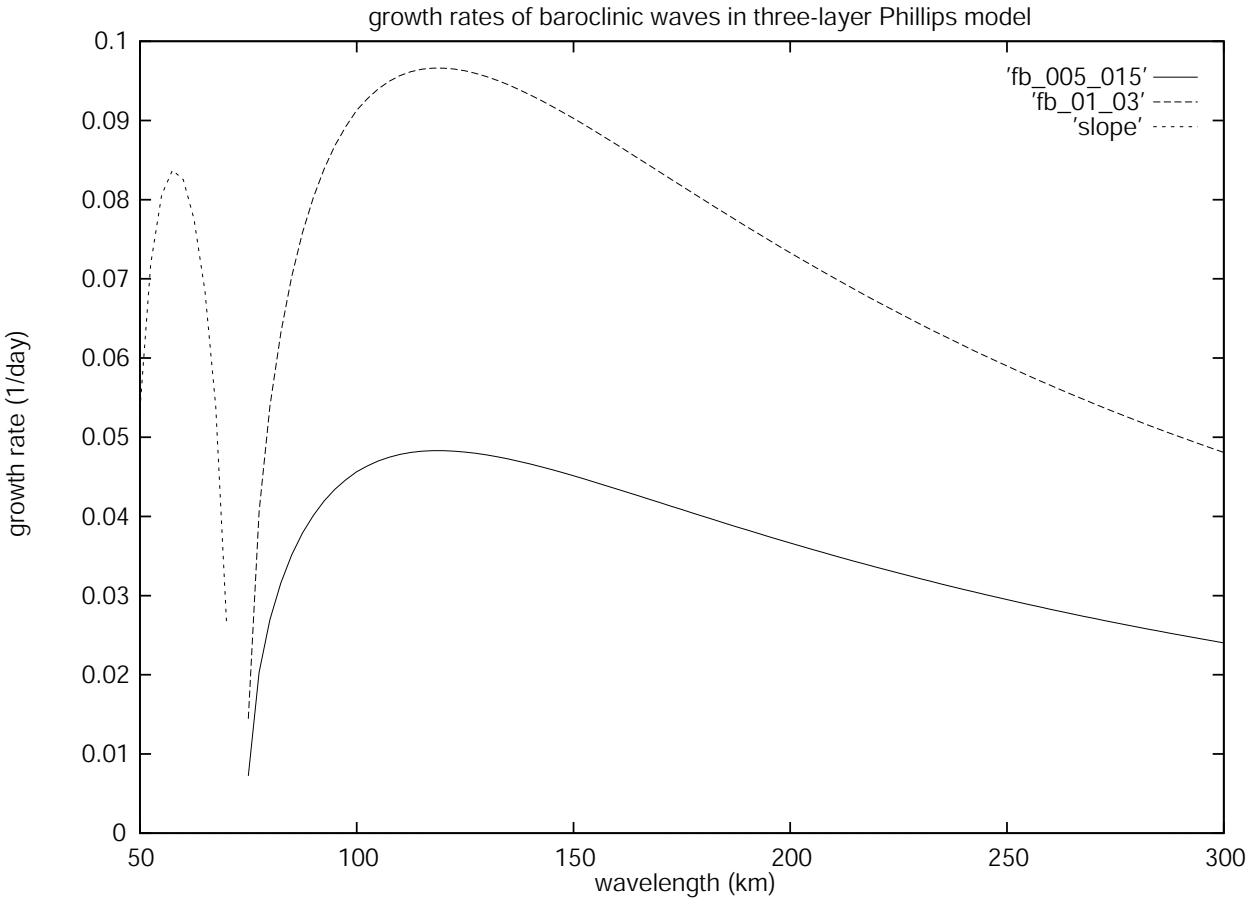

Figure 11: Growth rates of most unstable baroclinic waves for the three-layer Phillips problem calibrated on the PGW core. Two vertical shears of velocity are considered over flat bottom and the latter is used over a constant bottom slope similar to the real one.

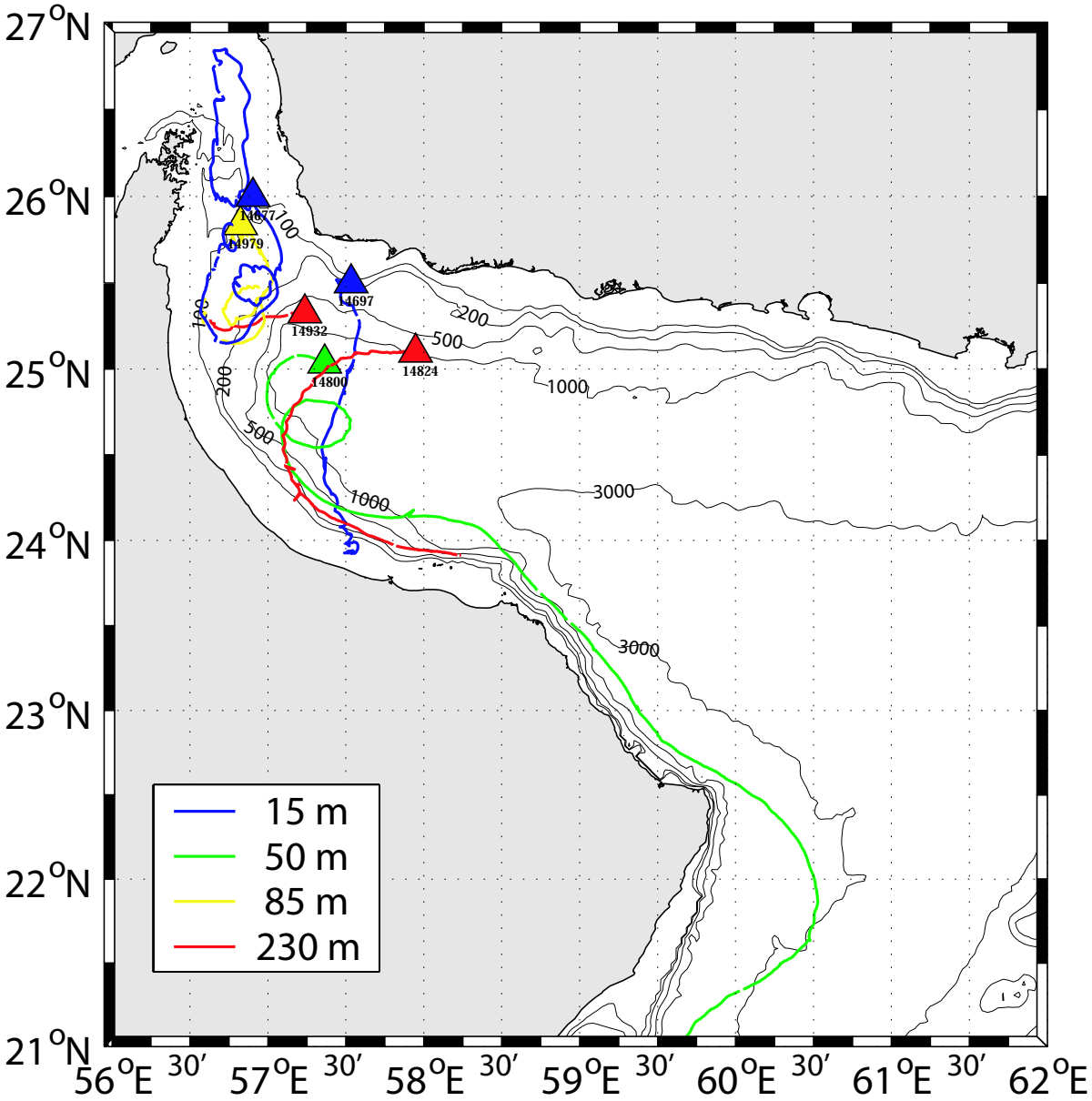

Figure 12: Surdrift buoy trajectories. Triangles indicate deployment position and colors give the drogue depth. Number of days of valid data is given in Table 2.

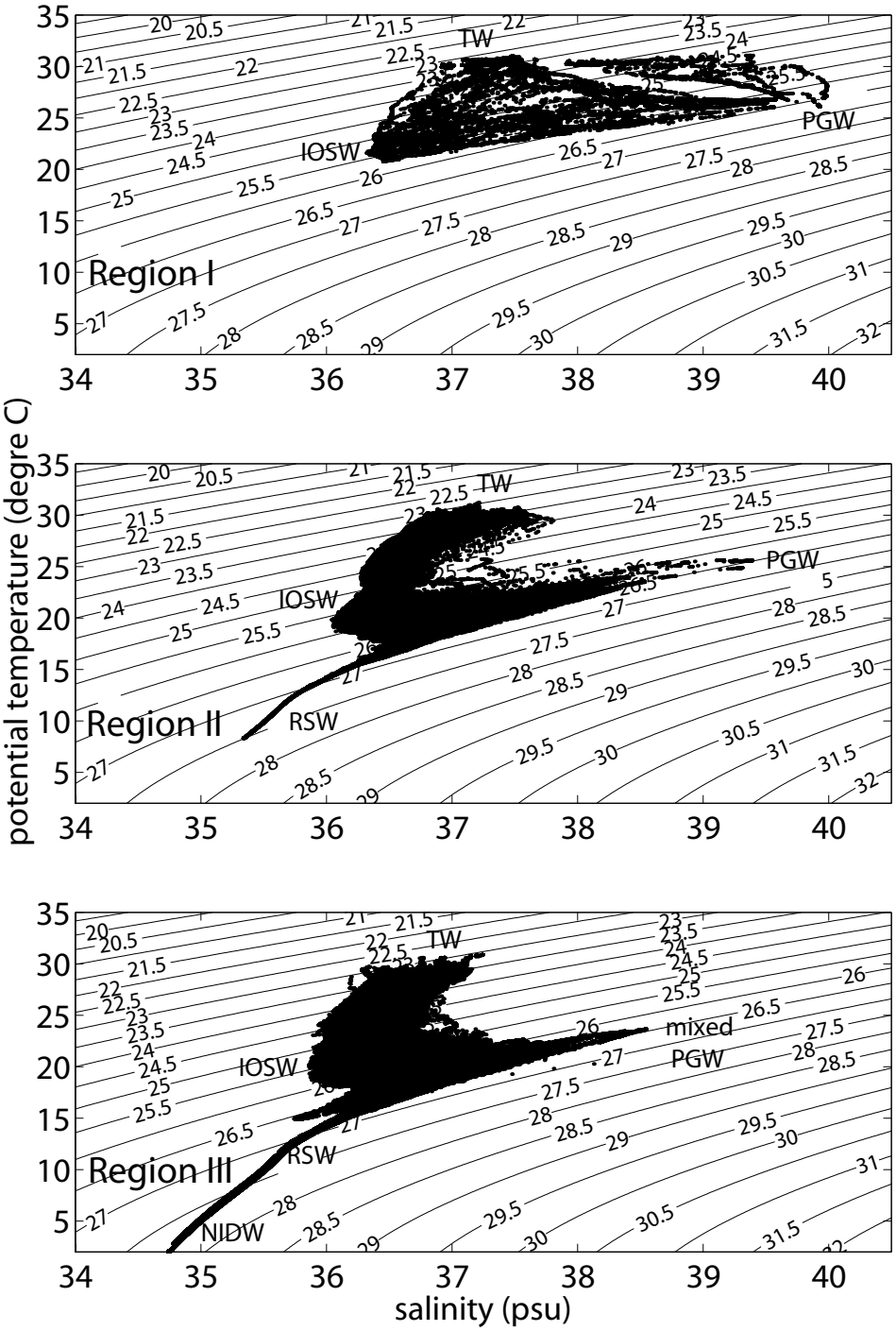

Figure 13: T-S diagram in the Strait of Hormuz and in the Gulf of Oman from GOGP99 data. Data has been gathered in three regions (see figure 1 for location).

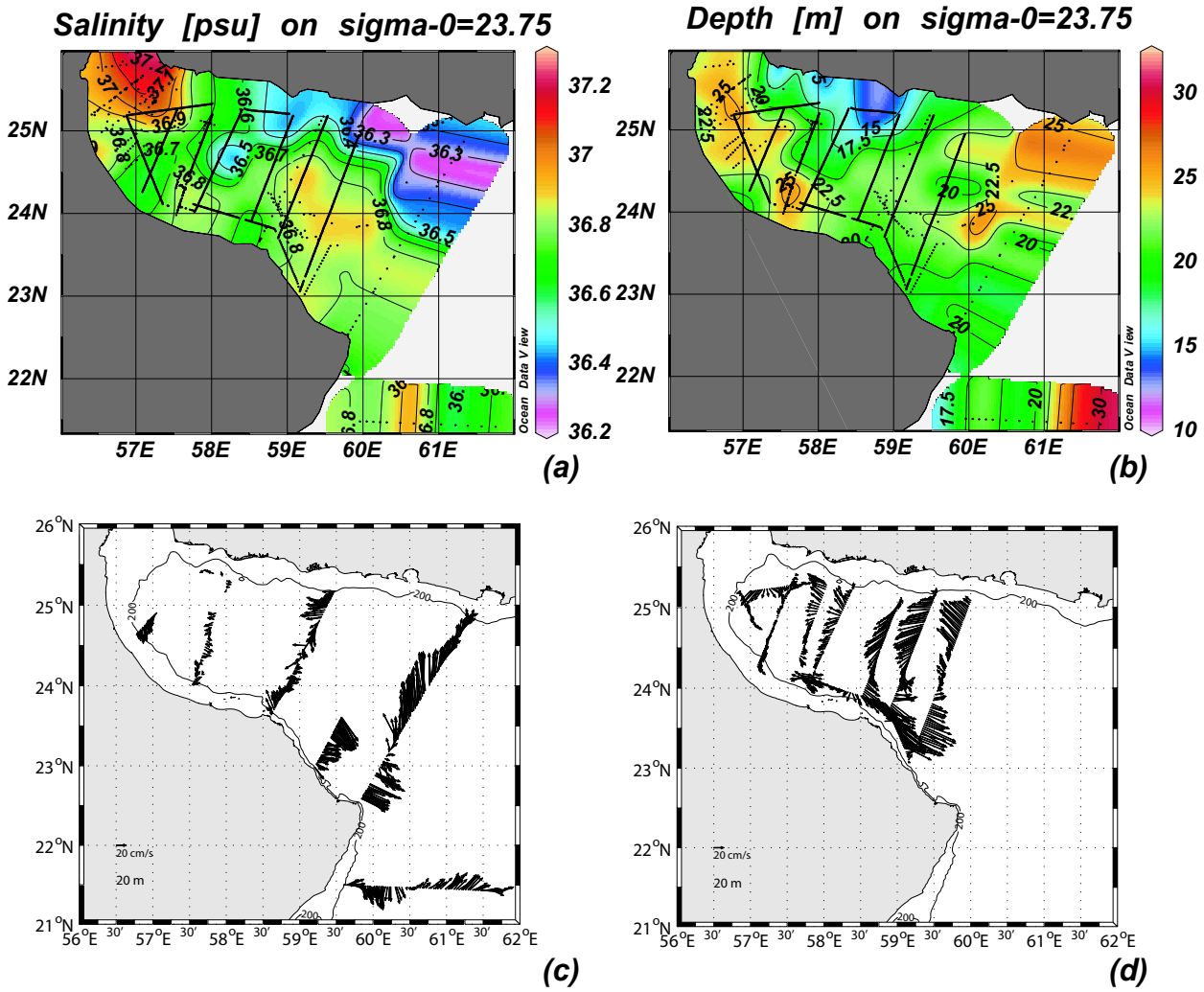

Figure 14: (a) Salinity map on the isopycnic surface $\sigma_0 = 23.75$ (at the base of the seasonal thermocline) based on synthesis of GOGP data, (c) depth of the isopycnic surface, (c) SADCP velocity vectors at 20 m depth, averaged over 15 minutes, during CTD-LADCP survey (Oct.8-13 for all sections except R01 on Nov.10), (d) same as (c) during Seasoar survey (Oct.21-Nov.1).

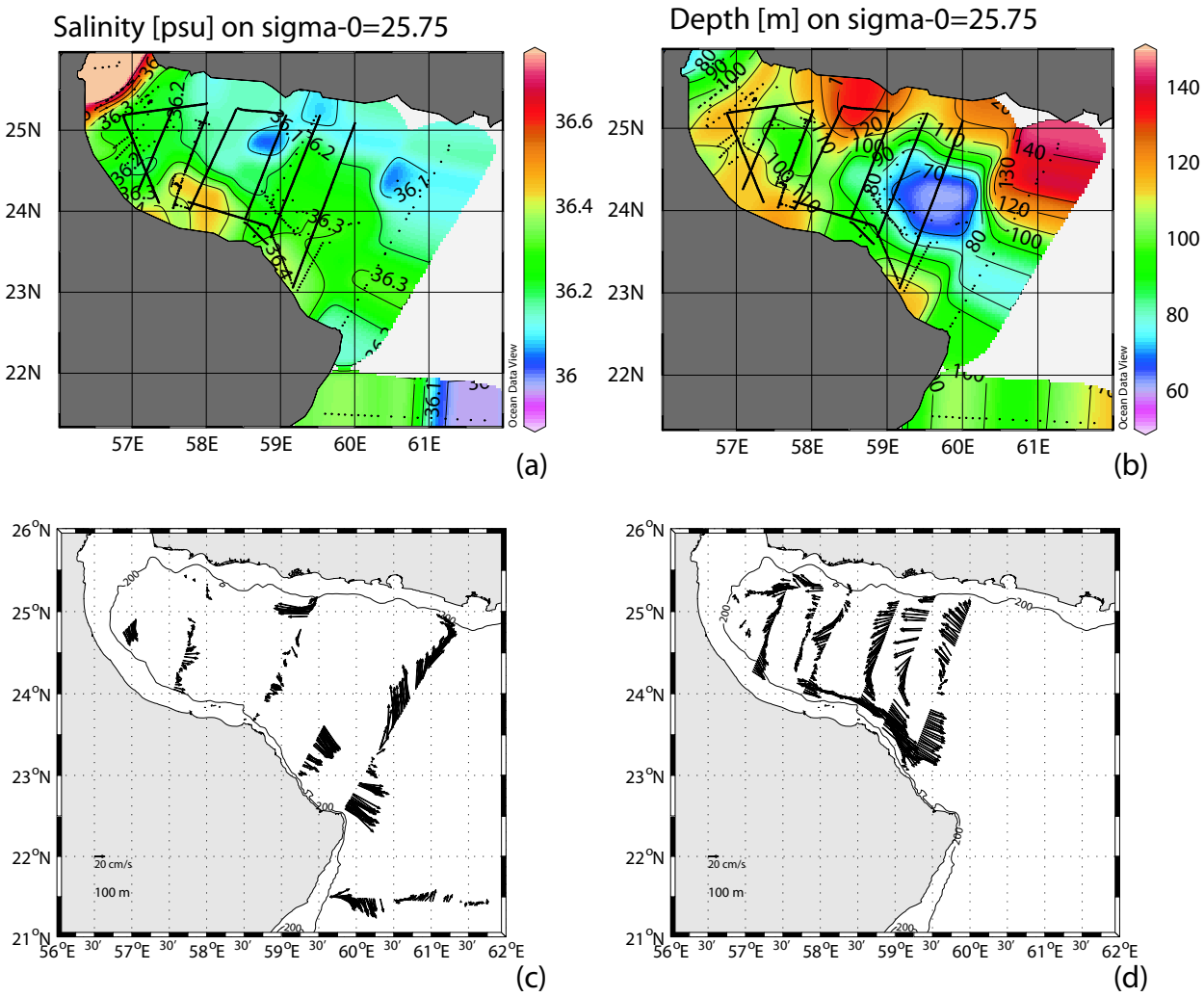

Figure 15: identical to figure 14 for water masses on the isopycnic surface $\sigma_0 = 25.75$ and flow at 100 m depth.

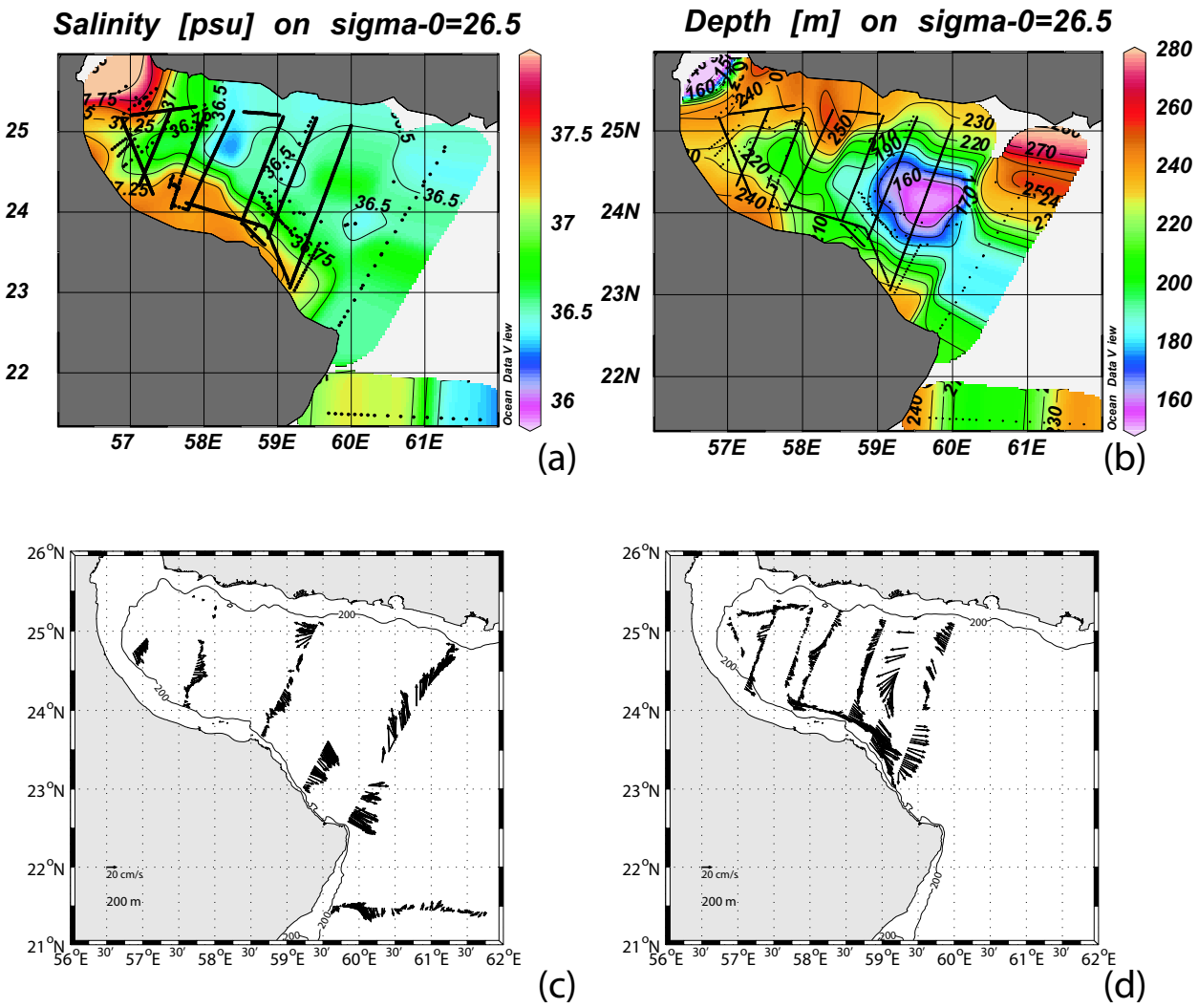

Figure 16: identical to figure 14 for water masses on the isopycnic surface $\sigma_0 = 26.5$ and flow at 200 m depth.

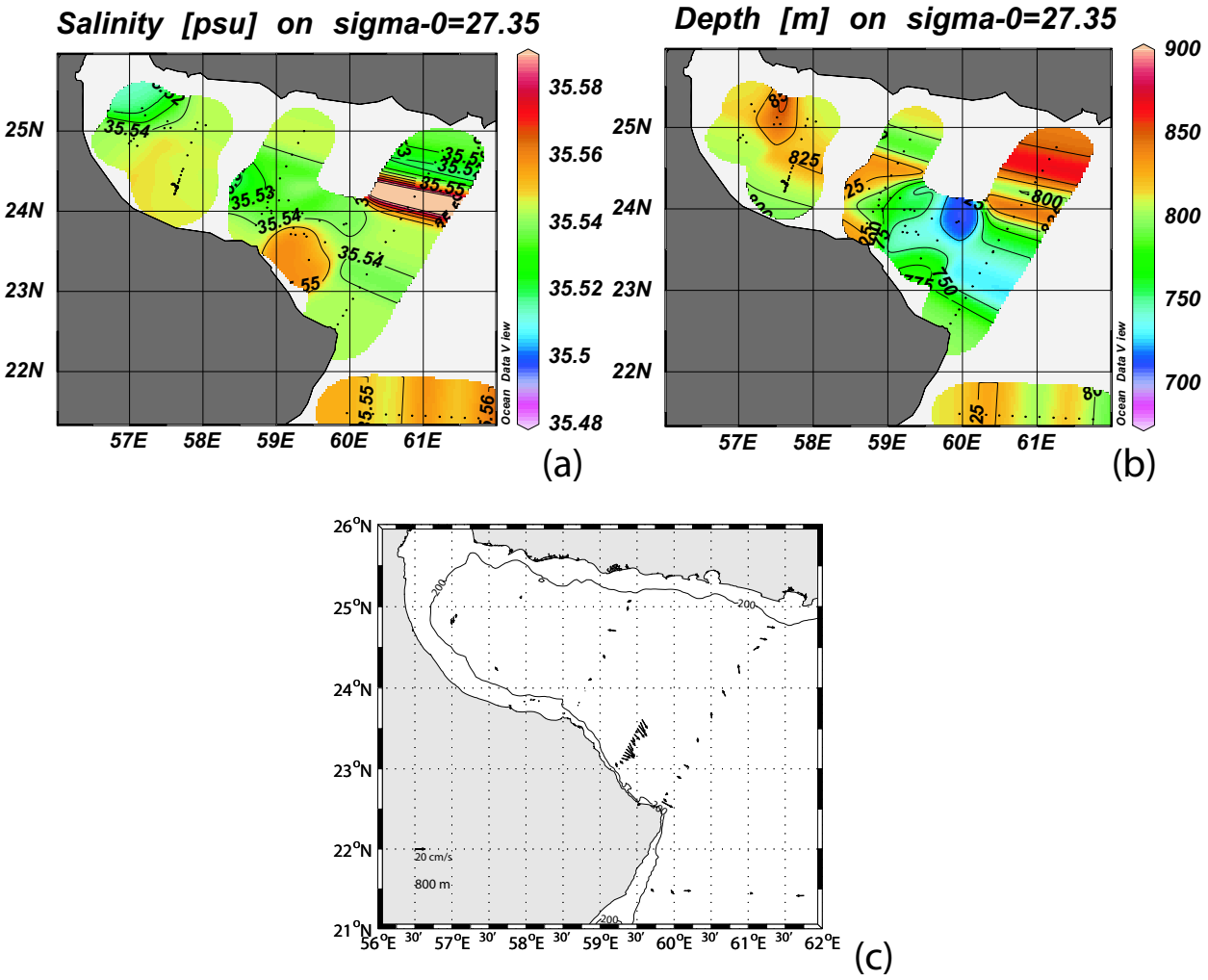

Figure 17: (a) Salinity map on the isopycnic surface $\sigma_0 = 27.35$, (b) depth of the isopycnic surface , (c) LADCP velocity vectors at the same depth, averaged over 15 minutes, during CTD-LADCP survey (Oct.8-13 for all sections except R01 on Nov.10).

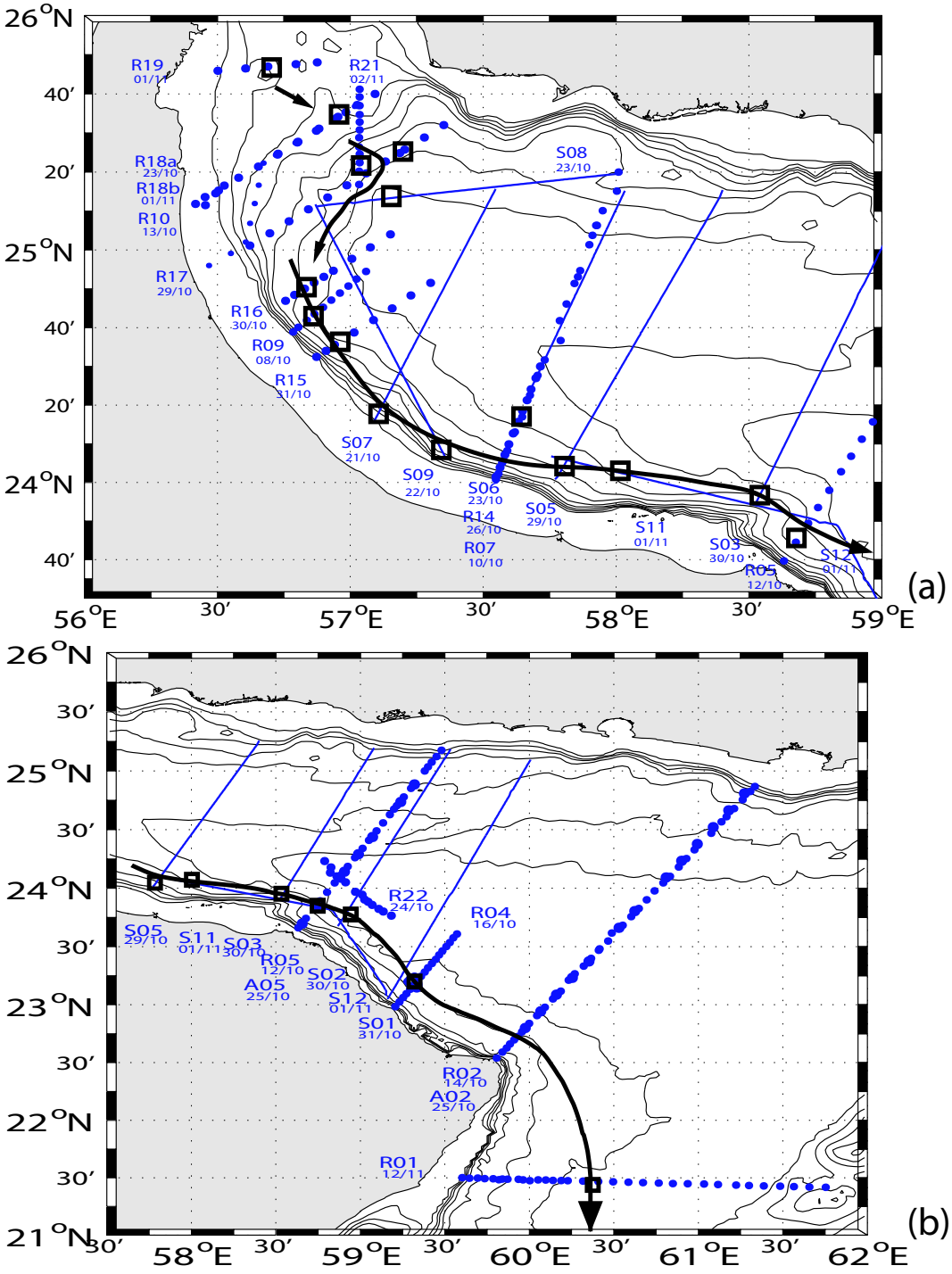

Figure 18: (a) Transect names, positions and dates in the western part of the Gulf of Oman. Black square locates salinity maximum in the PGW core. Black arrows sketch the PGW paths in this part of the Gulf, (b) Same as figure 15a, in the estern part of the Gulf of Oman.

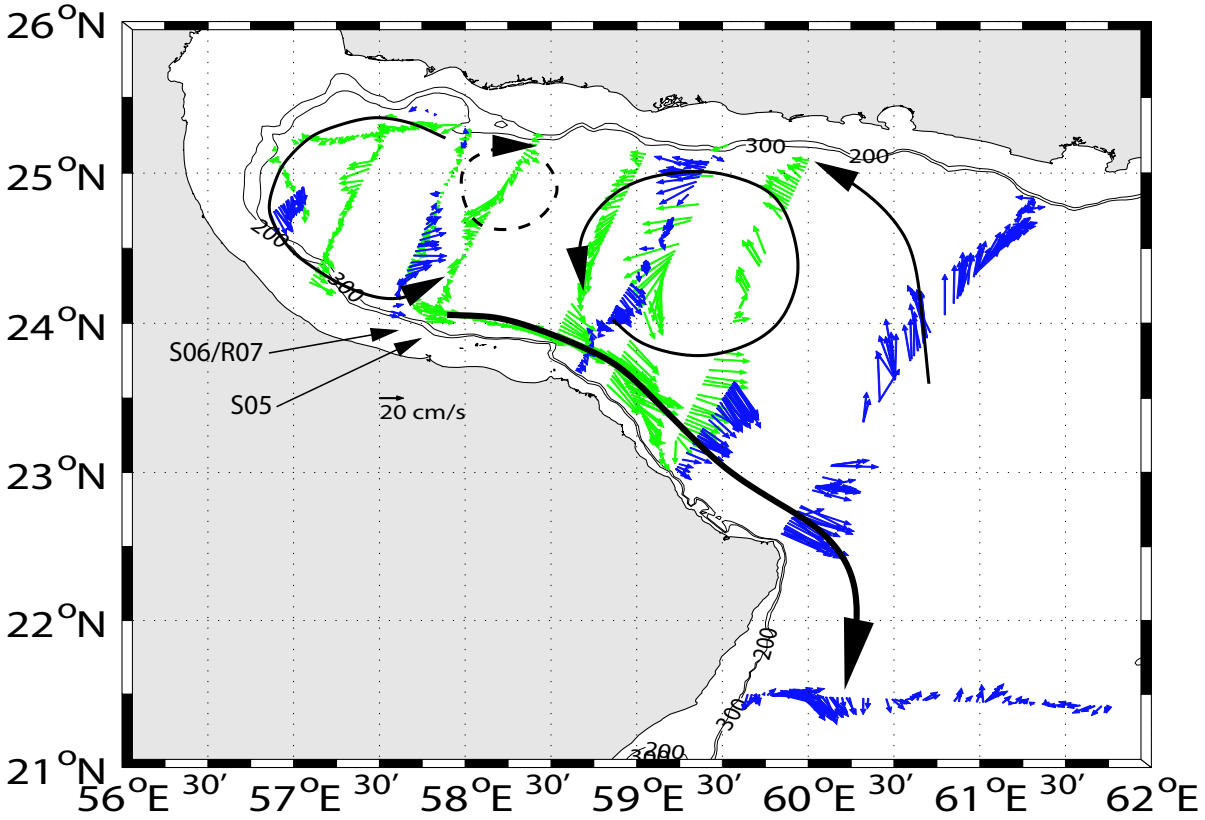

Figure 19: Regional circulation in the Gulf of Oman (upper 300 meters) sketched on the SADCP current at 200m.